Bose-Einstein Correlations in multi-hadronic Z^0 Decays

Diplomarbeit

zur Erlangung des Grades eines Magisters
an der Naturwissenschaftlichen Fakultät
der Leopold-Franzens-Universität Innsbruck

eingereicht von
Andreas Wildauer
im Jänner 2003

durchgeführt am Institut für Experimentalphysik
bei Univ.-Doz. Dr. Gerald Rudolph

Acknowledgements - Danksagung

Als erstes danke ich Herrn Univ. Doz. Dr. Gerald Rudolph für die kompetente und umfangreiche Betreuung die er von Anfang bis zum Ende der Arbeit leistete.

Herrn Prof. Dr. Dietmar Kuhn gilt besonderer Dank für sein großes Engagement der Gruppe und speziell den Diplomanden gegenüber.

Dank geht auch an Herrn Dr. Emmerich Kneringer, dessen positive Schuld es ist, daß ich im Laufe meines Studiums in die Teilchenphysik rutschte.

Zu guter letzt geht noch ein Dankeschön an die ganze Gruppe, in der man sich eigentlich nur wohl fühlen kann.

Spezieller Dank gilt natürlich auch meiner Familie:

Meinen Eltern und Großeltern für die finanzielle Unterstützung, die das Studentenleben um einiges erleichterte.

Meinem Bruder und meiner Mutter für die gratis Verleihung ihrer Autos, mit denen die Uni im Winter etwas komfortabler zu erreichen war als mit dem Fahrrad ...

Meiner Freundin Mirijam gilt besonderer Dank, weil sie sich ausgerechnet für mich entschieden hat.

Ach ja, und natürlich auch ein Dank an die zwei Typen, mit denen ich mir ein Büro teilen durfte ;-)

Contents

List of Figures

Chapter 1

Introduction and Motivation

In a head on collision of an accelerator experiment two particles collide with a certain center of mass energy E_{cm}. For this study the particles are leptons (e^+, e^-) and the energy is set to 91.2 GeV, which is roughly the rest mass of the Z^0 boson. When the leptons collide, three possible processes can occur. Two of them are elastic e^+e^- scattering (Bhabha scattering) and inelastic e^+e^- scattering where both virtual photons interact and produce hadrons. The third is the annihilation of e^+e^- into an intermediate particle: a photon, Z^0 boson or even a mixture of both.

If e^+e^- annihilates into an intermediate particle, at $E_{cm} = M_Z$, the one into a Z^0 is preferred (see section 2.2.3). With a probability of about 30% the Z^0 decays into two leptons, either a $\nu\bar{\nu}$, $\mu^+\mu^-$, $\tau^+\tau^-$ or again a e^+e^- pair, and with about 70% probability the Z^0 decays into a $q\bar{q}$ (quark-antiquark) pair which further on evolves into a final hadronic state[1]. This hadronic channel is subject of this study.

During the evolution of e^+e^- to hadrons many different physical processes take place. Unfortunately, the only things that can be measured, or about which the experimentalists can be quite sure, is the very initial state (electron-positron pair) and the very final state (lots of neutral and charged particles). With this information at hand it is the aim of particle physics to reveal the processes which take place during the transition from initial to final state. The theory which attempts to describe all this is the so called standard model of particle physics.

Due to the complexity of the seemingly basic process $e^+e^- \rightarrow hadrons$ it takes the whole *power* of the standard model to describe all stages from initial to final state and to reproduce the measured event topologies and other quantities by means of Monte Carlo simulations. A consequence of this probabilistic treatment is that some properties or processes which take place and are measured elude themselves from being described or reproduced. The Bose-Einstein effect, which is a purely quantum mechanical effect, is an example.

Even though the BE effect may play a minor role for most studies of multihadronic Z^0 decays, it is a good place to test suitable algorithms to describe it. Event topologies at the Z^0 peak are complex but not as complex as for fully hadronic W^+W^- decays or even events which result from proton antiproton collisions (at Fermilab for example). For those studies, BE effects are more important. For the first (W^+W^- decays), because the BE effect may introduce an unknown shift on the calculation of the W mass, for the second ($p\bar{p}$ collisions) because way more identical bosons, which underly the BE effect, are produced. Algorithms which describe BE effects in multihadronic Z^0 decays are also thought of being capable to describe the effect when it comes to W^+W^- decays or even $p\bar{p}$ events.

Chapter 2 gives an overview of the process of interest ($e^+e^- \rightarrow hadrons$) and of the theories

behind the different stages. In chapter 3 the experimental setup is presented and relevant aspects of the detector are discussed. A brief introduction to the theory of the BE effect and a sensitive quantity to measure it ($\rightarrow$ Q-distribution) is given in chapter 4. Analysis related things, i.e. event selection and the measured Q-distribution, are presented in chapter 5. Chapter 6 gives a theoretical overview of the two basic methods, namely PYBOEI (BE routine of PYTHIA) and a model by V.Kartvelishvili and R.Kvatadze, used to implement BE effects into MC simulations. How the algorithms are applied and results for all used variations of the basic methods can be read in chapter 7 and chapter 8 presents an application of the BE algorithm PYBOEI on 2, 3 and 4 jet topologies. Finally chapter 9 gives a summary of what has been done.

Chapter 2

Theoretical Framework

2.1 The Process $e^+e^- \rightarrow Z^0 \rightarrow q\bar{q}$

In the case of a hadronic event the evolution from the initial state e^+e^- to the final hadronic state can be subdivided into different processes (see Figure 2.1).
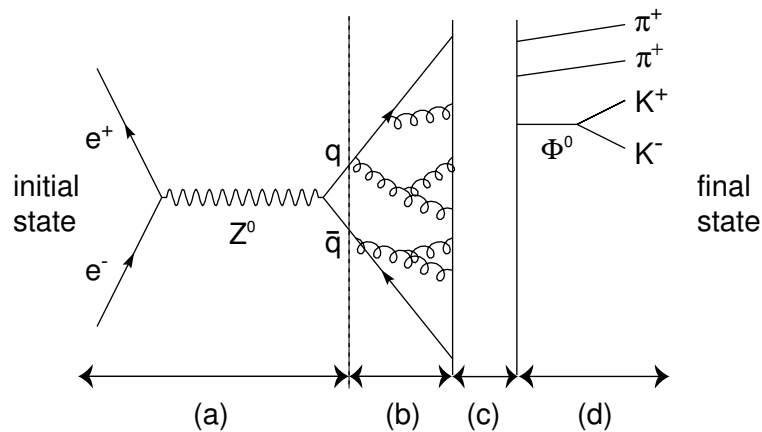
Figure 2.1: Schematic representation of the process $e^+e^- \rightarrow hadrons$

(a) Collision and annihilation of the two leptons e^+e^- into a Z^0 boson which decays further into a primary $q\bar{q}$ pair. This process is well described by electro-weak theory.

(b) Fragmentation (perturbative region): radiation of gluons from the primary $q\bar{q}$ pair, gluon splitting

(c) Fragmentation (non-perturbative region): transition of partons (i.e. quarks and gluons) into colorless hadrons

(d) Decay of short lived hadrons

The terms hadronization and fragmentation are used differently throughout particle physics. In this thesis hadronization stands for the complete process of evolution from the primary quark pair to the final state particles including the decay of short lived particles. Fragmentation is a

subprocess of hadronization, i.e. the perturbative region (b) and the non-perturbative region (c) of figure (2.1). The whole process can be described by the so called standard model of particle physics. The theoretical basis is presented in the next section.

2.2   The Standard Model

The Standard Model is the most successful theory in today's particle physics. It attempts to describe fundamental particles and the forces that act between them.

According to the standard model 24 fundamental particles, which are all fermions (spin $\frac{1}{2}$), and 12 "messenger particles", (all bosons, spin = 1) which are supposed to mediate the different kind of forces between particles, exist. Fermions are further divided into 6 leptons and 6 quarks (see table 2.1). Since each quark carries color charge (red, green or blue), 18 different quarks exist.

Generation	I	II	III	Charge
Leptons	$\begin{pmatrix} \nu_e \\ e^- \end{pmatrix}$	$\begin{pmatrix} \nu_\mu \\ \mu^- \end{pmatrix}$	$\begin{pmatrix} \nu_\tau \\ \tau^- \end{pmatrix}$	0 −1
Quarks	$\begin{pmatrix} u \\ d \end{pmatrix}$	$\begin{pmatrix} c \\ s \end{pmatrix}$	$\begin{pmatrix} t \\ b \end{pmatrix}$	2/3 −1/3

Table 2.1: Fundamental fermions of the standard model

Of the 4 known fundamental forces - electromagnetic, weak, strong and gravitational - "only" the first 3 are part of the standard model. It was not yet possible to describe all four forces in one theory, although many attempts were/are made ($\rightarrow$ Grand Unified Theories [3]). Reasons for that are eclectic and complicated and might be read elsewhere[3]. However, since gravity is by far the weakest of all forces (see Table 2.2), it does not play a role for the outcome of present particle physics experiments and can therefore be neglected in the study of the other three interactions.

interaction	mediator(s)	range [m]	relative strength
strong	8 gluons	10^{-15}	1
electromagnetic	photon (γ)	∞	1/137
weak	$W^\pm$, Z^0	10^{-17}	10^{-5}
gravitational	graviton (postulated)	∞	10^{-39}

Table 2.2: Fundamental interactions and their relative strength[4, 5]

Within the standard model electromagnetic and weak force are described by electro-weak theory, strong interactions by quantum chromo dynamics (QCD).

2.2.1 Electro-weak Theory

The formal unification of *quantum electro dynamics* (QED) and the theory of *weak interactions* into a theory of *electro-weak interactions* was done by Glashow, Salam and Weinberg in 1967. This section and the next were written in analogy to [4, 5].

Electro-weak theory is based on the gauge group $SU(2)_L \times U(1)_Y$. For free electrons and neutrinos the Lagrangian looks like

$$\mathcal{L} = \imath(\bar{\Psi}_e\gamma^\mu\partial_\mu\Psi_e) + \imath(\bar{\Psi}_{\nu L}\gamma^\mu\partial_\mu\Psi_{\nu L}) \tag{2.1}$$

No right handed neutrinos have ever been observed and hence no right handed term for neutrinos appears in the Lagrangian. The electron spinor can be split into a right and a left handed part

$$\Psi_e = \Psi_{eR} + \Psi_{eL} \tag{2.2}$$

and (2.1) can be written in a more symmetric form

$$\mathcal{L} = \imath(\bar{\Psi}_{\nu L}, \bar{\Psi}_{eL})\gamma^\mu\partial_\mu \begin{pmatrix} \Psi_{\nu L} \\ \Psi_{eL} \end{pmatrix} + \imath(\bar{\Psi}_{eR}\gamma^\mu\partial_\mu\Psi_{eR}) \tag{2.3}$$

In order to keep the first part of (2.3) gauge invariant under a transformation $U(x) \in SU(2)$, ∂_μ needs to be replaced by the covariant derivative D_μ

$$\partial_\mu \to D_\mu = \partial_\mu + \imath g \sum_{k=1}^{3} \frac{1}{2} W_\mu^k \sigma_k \tag{2.4}$$

The interaction term of the new gauge invariant Lagrangian is

$$\mathcal{L}_W = -\frac{g}{2}(\bar{\Psi}_{\nu L}, \bar{\Psi}_{eL})\gamma_\mu W_\mu^k \sigma_k \cdot \begin{pmatrix} \Psi_{\nu L} \\ \Psi_{eL} \end{pmatrix} \tag{2.5}$$

where $\sigma_{k=1,2,3}$ denote the three generators of SU(2) (i.e. Pauli matrices) and $W_\mu^{k=1,2,3}$ are the three gauge fields with gauge bosons $W^{1,2,3}$. With $W^\pm := \frac{1}{\sqrt{2}}(W^1 \mp \imath W^2)$ and substitution of the Pauli matrices a preliminary result for the electro-weak Lagrangian is given by

$$\mathcal{L}_W = -\frac{g}{2} \cdot (W_\mu^3(\bar{\Psi}_{\nu L}\gamma^\mu\Psi_{\nu L} - \bar{\Psi}_{eL}\gamma^\mu\Psi_{eL})$$
$$\underbrace{-\frac{g}{\sqrt{2}} \cdot W_\mu^+(\bar{\Psi}_{\nu L}\gamma^\mu\Psi_{eL}) - \frac{g}{\sqrt{2}} \cdot W_\mu^-(\bar{\Psi}_{eL}\gamma^\mu\Psi_{\nu L})}_{=: \mathcal{L}_{CC}} \tag{2.6}$$

The coupling of $W^\pm$ in $\mathcal{L}_{CC}$ is identical to the charged-current coupling in weak theory, and hence $W^\pm$ are identified as the two charged gauge bosons of weak interactions.

To get a connection to Z^0 and the gauge boson A of QED, (2.3) is also made invariant under a $U(1)$ transformation.

Again D_μ is replaced and, with the following currents

$$\jmath_\nu^\mu = \bar{\Psi}_{\nu L}\gamma^\mu\Psi_{\nu L}$$
$$\jmath_{eL}^\mu = \bar{\Psi}_{eL}\gamma^\mu\Psi_{eL}$$
$$\jmath_{eR}^\mu = \bar{\Psi}_{eR}\gamma^\mu\Psi_{eR}$$
$$\jmath_{em}^\mu = \bar{\Psi}_e\gamma^\mu\Psi_e = \jmath_{eL}^\mu + \jmath_{eR}^\mu$$

it is possible to write down the complete interaction term of the electro-weak Lagrangian

$$\begin{aligned}\mathcal{L}_W =& \mathcal{L}_{CC} - \frac{1}{2}(gW_\mu^3 - g'B_\mu)\jmath_\nu^\mu \\ &+ \frac{1}{2}(gW_\mu^3 + g'B_\mu)\jmath_{eL}^\mu - Y_R g' B_\mu \jmath_{eR}^\mu\end{aligned} \tag{2.7}$$

where Y_R is the so called hypercharge.

Since both, W^3 and B, couple to the neutrino, none can be the photon. However, the linear combination $(gW_\mu^3 - g'B_\mu)$ couples to the neutrino only and since the neutrino feels nothing but a weak force this term can be identified with the Z^0 boson. The gauge field A_μ for the photon is an orthogonal linear combination to the Z^0

$$\begin{aligned}A_\mu &= B_\mu \cos\theta_W + W_\mu^3 \sin\theta_W \\ Z_\mu^0 &= -B_\mu \sin\theta_W + W_\mu^3 \cos\theta_W\end{aligned} \tag{2.8}$$

with $\cos(\theta_W) = \frac{g}{\sqrt{g^2+g'^2}}$ and $\sin(\theta_W) = \frac{g'}{\sqrt{g^2+g'^2}}$.

The observed gauge bosons Z^0 and A are a mixture of the gauge fields obtained by requiring gauge invariance of (2.3). The mixing angle θ_W is called Weinberg angle. It needs to be determined by experiment and has been measured to $\sin^2\theta_W = 0.2315 \pm 0.0002$[5]. With the new fields Z_μ^0 and A_μ (2.7) becomes

$$\begin{aligned}\mathcal{L}_W =& \mathcal{L}_{CC} \\ &- \sqrt{g^2+g'^2} \cdot Z_\mu \cdot \{\frac{1}{2}\jmath_\nu^\mu - \frac{1}{2}\jmath_{eL}^\mu - \sin^2\theta_W(-\jmath_{eL}^\mu + Y_R\jmath_{eR}^\mu)\} \\ &- \sqrt{g^2+g'^2} \cdot \sin\theta_W \cos\theta_W \cdot A_\mu(-\jmath_{eL}^\mu + Y_R\jmath_{eR}^\mu)\end{aligned} \tag{2.9}$$

It is possible to convert the last term to the well known interaction term of electromagnetism by choosing the (up to now) arbitrary hypercharge Y_R to -1 and identifying the electric charge with $e = \sqrt{g^2+g'^2} \cdot \sin\theta_W \cdot \cos\theta_W$.

So, at length, the interaction term of the final Lagrangian of electro-weak theory is

$$\mathcal{L}_W = \mathcal{L}_{CC} + eA_\mu \cdot \jmath_{em}^\mu - \frac{e}{\sin\theta_W \cos\theta_W} \cdot Z_\mu \jmath_{NC}^\mu \tag{2.10}$$

with $\jmath_{NC}^\mu = (\frac{1}{2}\jmath_\nu^\mu - \frac{1}{2}\jmath_{eL}^\mu) + \sin^2\theta_W \jmath_{em}^\mu$.

This Lagrangian is valid for the 3 lepton isospin-doublets (ν_e, e^-), (ν_μ, μ^-) and (ν_τ, τ^-). In order to expand this scheme to suite the 3 quark generations as well, the first part of $\jmath_{NC}$ is rewritten as a sum of a left and a right handed part

$$\jmath_{NC} = (I_3 - Q\sin^2\theta_W)\jmath_L - Q\sin^2(\theta_W)\jmath_R \tag{2.11}$$
$$= C_L\jmath_L + C_R\jmath_R \tag{2.12}$$

If the three quark generations are also understood as weak isospin doublets, i.e. $I_3(u) = 1/2$ and $Q(u) = 2/3$, one can easily calculate the appropriate neutral current $\jmath_{NC}$ and $\mathcal{L}_W$ for all quarks (see table 2.3).

fermion	charge Q	isospin I_3	$C_L =$ $I_3 - Q \sin^2 \theta_W$	$C_R =$ $-Q \sin^2 \theta_W$
ν_e, ν_μ, ν_τ	0	1/2	1/2	0
e^-, μ^-, τ^-	-1	-1/2	$-1/2 + \sin^2 \theta_W$	$\sin^2 \theta_W$
u, c, t	2/3	1/2	$1/2 - (2/3) \sin^2 \theta_W$	$-(2/3) \sin^2 \theta_W$
d, s, b	-1/3	-1/2	$-1/2 + (1/3) \sin^2 \theta_W$	$(1/3) \sin^2 \theta_W$

Table 2.3: Coupling constants for the neutral current

Alternatively, v_f and a_f can be defined as

$$v_f = C_L + C_R$$
$$a_f = C_L - C_R \tag{2.13}$$

to calculate the cross section of $e^+ e^- \to Z^0 \to f\bar{f}$ and are used in section 2.2.3.

The procedure shown is often presented as a unification of weak and electromagnetic theory. Rather it is a unified formulation of both theories. The value of the parameter Y_R was set to -1 to convert the last term of (2.9) to the known interaction term of electromagnetism. It is not an outcome of electro-weak theory. Neither is θ_W - it has to be determined by experiment.

2.2.2 The Higgs Mechanism

By requiring the Lagrangian (2.3) in the previous section to be gauge invariant, 3 new gauge bosons $W^{1,2,3}$ which lead to the observable particles W^+, W^- and Z^0 were introduced. In this theory these particles are, as well as the photon, massless. To generate the observed masses, a new physical assumption called *Higgs mechanism*[4, 5] was found. First, the basic mechanism which makes use of spontaneous breaking of a gauge symmetry is shown by the example of a complex scalar field. Second the full mechanism is demonstrated by generating a mass for a gauge boson of a $U(1)$ local gauge symmetry. Finally results for the more complex $SU(2)_L \times U(1)_Y$ symmetry of electro-weak theory and it's gauge bosons are presented.

Spontaneous Breaking of a Global U(1) Symmetry

Consider a complex scalar field Φ described by a Lagrangian

$$\mathcal{L} = (\partial_\mu \Phi)^* (\partial^\mu \Phi) - V \tag{2.14}$$

with the potential V as

$$V = \mu^2 (\Phi^* \Phi) + \lambda (\Phi^* \Phi)^2 \tag{2.15}$$

where $\mu^2 < 0$ and $\lambda > 0$. The Lagrangian (2.14) is invariant under a global $U(1)$ gauge transformation $\Phi \to e^{i\alpha}\Phi$. With $\Phi = 1/\sqrt{2}(\Phi_1 + i\Phi_2)$, (2.14) becomes

$$\mathcal{L} = \frac{1}{2}(\partial_\mu \Phi_1)^2 + \frac{1}{2}(\partial_\mu \Phi_2)^2 - \frac{1}{2}\mu^2(\Phi_1^2 + \Phi_2^2) - \frac{1}{4}\lambda(\Phi_1^2 + \Phi_2^2)^2 \tag{2.16}$$

There is an infinite number of minima for the potential $V(\Phi)$ which fulfill

$$\Phi_1^2 + \Phi_2^2 = -\frac{\mu^2}{\lambda} =: v^2 \tag{2.17}$$

Without loss of generality it is possible to move the field Φ to one arbitrary minimum, say $\Phi_1 = v$ and $\Phi_2 = 0$ and expand $\mathcal{L}$ about this minimum with two new fields η and ξ

$$\Phi(x) = \sqrt{\frac{1}{2}} \{v + \eta(x) + \imath\xi(x)\} \tag{2.18}$$

This translation of the field to one arbitrary minimum spontaneously breaks the symmetry of the Lagrangian. Substitution of (2.18) into (2.16) yields

$$\mathcal{L} = \frac{1}{2}(\partial_\mu \xi)^2 + \frac{1}{2}(\partial_\mu \eta)^2 + \mu^2 \eta^2 + const. + higher - terms \tag{2.19}$$

Even though this Lagrangian describes the same physics as the original one, it has a field η with a mass term μ^2. If compared to the Lagrangian of the familiar Klein Gordon equation, the mass of the particle described by η is $m_\eta = \sqrt{-2\mu^2}$. Unfortunately a second field ξ is also present which describes a massless particle. By the attempt of generating a massive boson by spontaneous symmetry breaking we also got an unwanted massless gauge boson, the so called *Goldstone Boson*. A hint for a solution to this problem can be seen if we chose the gauge symmetry to be local instead of global.

Higgs Mechanism for a Local U(1) Symmetry

If the Lagrangian (2.14) shall be invariant under a local gauge transformation like $\Phi \to e^{\imath\alpha(x)}\Phi$, the derivative ∂_μ has to be replaced by the covariant form D_μ

$$\partial_\mu \to D_\mu = \partial_\mu - \imath e A_\mu \tag{2.20}$$

and the gauge field A_μ transforms as

$$A_\mu \to A_\mu + \frac{1}{e}\partial_\mu \alpha(x) \tag{2.21}$$

The gauge invariant Lagrangian then becomes

$$\mathcal{L} = (\partial^\mu + \imath e A^\mu)\Phi^*(\partial_\mu - \imath e A_\mu)\Phi - \mu^2 \Phi^* \Phi - \lambda(\Phi^*\Phi)^2 - \frac{1}{4}F_{\mu\nu}F^{\mu\nu} \tag{2.22}$$

With the same procedure as before, i.e. expansion of Φ about one minimum of the potential V a.s.o., again a massless Goldstone particle enters the scene. This time, however, an unusual off-diagonal term $A_\mu \partial_\mu \xi$ appears which gives a hint that not all fields which appear in $\mathcal{L}$ give rise to an observable particle. Further on, the gauge boson A_μ acquires a mass $m_A = ev$ (see 2.25), which means it can be polarized longitudinal as well and its degrees of freedom increase from 2 to 3. This additional degree of freedom corresponds to the possibility to make an additional gauge transformation of the original Lagrangian.

With a different set of real fields (h, Θ), instead of (η, ξ), expand the field Φ about one minimum of the potential (2.15)

$$\Phi = \sqrt{\frac{1}{2}}(v + h(x))\, e^{\imath\Theta(x)/v} \tag{2.23}$$

and substitute it with an additional transformation of the gauge field

$$A_\mu \to A_\mu + \frac{1}{ev}\partial_\mu \Theta \tag{2.24}$$

into the original Lagrangian (2.22) and get

$$\mathcal{L} = \frac{1}{2} \left(\partial_\mu h^2 \right) - \lambda v^2 h^2 + \frac{1}{2} e^2 v^2 A_\mu^2 + selfint. + higher - order \tag{2.25}$$

At last, no Goldstone boson appears in this Lagrangian. It describes two massive particles, one gauge boson A_μ and the so called *Higgs boson h*. The Goldstone boson has been turned into the longitudinal polarization of the massive particle A_μ.

Higgs mechanism for electro-weak theory

To generate the masses of $W^\pm$, Z^0 and γ, the Higgs mechanism is applied on the $SU(2)_L \times U(1)_Y$ symmetry of electro-weak theory. The procedure is the same as presented in the preceding section, but more complicated in detail due to the more complex symmetry.

The basic potential is (2.14) with $\mu^2 < 0$ and $\lambda > 0$. Φ is a $SU(2)$ doublet of complex scalar fields

$$\Phi = \frac{1}{\sqrt{2}} \left(\begin{array}{c} \Phi_1 + \imath \Phi_2 \\ \Phi_3 + \imath \Phi_4 \end{array} \right) \tag{2.26}$$

This Φ is the original one used by Weinberg in 1967. The potential (2.14) has minima at

$$\Phi_1^2 + \Phi_2^2 + \Phi_3^2 + \Phi_4^2 = -\frac{\mu^2}{\lambda} =: v^2 \tag{2.27}$$

The choice of a certain minimum Φ_0 is arbitrary since any will break the symmetry and create masses for the gauge bosons. Knowing that the photon is massless, Φ_0 is taken as

$$\Phi_0 = \frac{1}{\sqrt{2}} \left(\begin{array}{c} 0 \\ v \end{array} \right) \tag{2.28}$$

This choice breaks both symmetries $SU(2)$ and $U(1)_Y$ but leaves the subgroup $U(1)_{em}$ unbroken and therefore the corresponding gauge boson γ will be massless.

The masses of $W^\pm$ and Z^0 are obtained by substituting (2.28) into the Lagrangian of electro-weak theory and come out as

$$M_\gamma = 0 \qquad\qquad M_{Z^0} = \frac{1}{2} v \sqrt{g^2 + g'^2}$$
$$M_{W^\pm} = \frac{1}{2} vg \tag{2.29}$$

v is also called the vacuum expectation value of the Higgs boson.

With $v = 246$ GeV, $\sin(\theta_W)^2 = 0.2315$, $e = \sqrt{4\pi\alpha_{e.m.}(M_Z)}$, $\alpha_{e.m.}(M_Z) \approx 1/128$ and $e = g\sin(\theta_W) = g'\cos(\theta_W)$, numerical values for the masses are

	Z^0	$W^\pm$
Higgs	$\approx 91 GeV$	$\approx 80 GeV$
experiment	$91.1876 \pm 0.0021 GeV$	$80.423 \pm 0.039 GeV$

Table 2.4: Calculated and measured masses of electro-weak gauge bosons [1]

M_W and M_Z are not predicted by the Higgs mechanism, because v and s_W^2 are input values coming from experiment. What is predicted is a relation between the masses of the gauge bosons: $\frac{M_W}{M_Z} = \cos\theta_W$. With the Higgs mechanism it is also possible to generate the masses of leptons and quarks[5]. The Higgs particle H^0 is the only missing element of the standard model to date.

2.2.3 The Cross Section of $e^+e^- \to f\bar{f}$

By use of electro-weak theory it is possible to calculate the cross section of $e^+e^- \to f\bar{f}$ for all possible intermediate particles (i.e. γ, Z^0 or interference γ/Z^0) and final fermions (i.e. e, μ, τ, d, u, s, ...)[6]. It is given by

$$\frac{d\sigma}{d\Omega} = \frac{\alpha_{em}^2}{4S} \left[G_1 \cdot (1 + \cos^2\theta) + 2G_2 \cdot \cos\theta \right] \tag{2.30}$$

where θ is the angle between incoming electron and outgoing fermion and

$$G_1 = Q_f^2 - 2 \cdot Q_f S \cdot \Re(1/D) \cdot v_e v_f + \frac{S^2}{|D|^2}(v_e^2 + a_e^2)(v_f^2 + a_f^2)$$

$$G_2 = 0 - 2 \cdot Q_f S \cdot \Re(1/D) \cdot a_e a_f + \frac{4S^2}{|D|^2}(v_e a_e)(v_f a_f)$$

$$D = (S - M_Z^2) + \imath M_Z \Gamma_Z \qquad S = E_{cm}^2 \tag{2.31}$$

The first part in $G_{1/2}$ stands for annihilation into a γ, the second for the possible interference γ/Z^0 and the third for a Z^0 only. The couplings of the fermions to the Z^0 can be deduced by looking at table (2.3) and at

$$v_f = \frac{I_3 - 2Q_f \sin^2\theta_W}{2\sin\theta_W \cos\theta_W} \qquad\qquad a_f = \frac{I_3}{2\sin\theta_W \cos\theta_W} \tag{2.32}$$

Γ_Z is the total decay width of the Z^0 and has the numerical value of 2.4952 ± 0.0023 GeV[1].

To get the total cross section σ_{tot}, integrate (2.30) over $d\Omega = \sin\theta d\theta d\phi$. The result is

$$\sigma_{tot} = \frac{4\pi\alpha^2}{3S} \cdot G_1 = \sigma_0 \cdot G_1 \tag{2.33}$$

A closer look at G_1 reveals that the interference term γ/Z^0 vanishes, since $\Re(1/D) = 0$ for $S = M_Z^2$. Annihilation into a Z^0 boson is preferred by that into a γ by

$$\sigma_{e^+e^- \to \gamma \to q\bar{q}} = \sigma_0 \cdot \sum_q Q_q^2 = \frac{11}{9}\sigma_0$$

$$\sigma_{e^+e^- \to Z^0 \to q\bar{q}} = \sigma_0 \frac{S}{\Gamma_Z^2}(v_e^2 + a_e^2) \cdot \sum_q (v_q^2 + a_q^2) \approx 1296\sigma_0$$

$$\Rightarrow \frac{\sigma_\gamma}{\sigma_{Z^0}} \approx 1 : 1060$$

See table (2.5) for detailed decay probabilities of the Z^0 into the possible fermions: $\nu\bar{\nu}$, e^+e^-, $\mu^+\mu^-$, $\tau^+\tau^-$ and $u\bar{u}$, $c\bar{c}$, $d\bar{d}$, $s\bar{s}$ or $b\bar{b}$. No decay into a $t\bar{t}$ is expected because the center of mass energy ($E_{cm} = 91.2$ GeV) is too low for t-quark production which has a mass of about $175\frac{GeV}{c^2}$[1].

fermion	prob.	$\sum$
$\nu_e \bar{\nu}_e$, $\nu_\mu \bar{\nu}_\mu$ or $\nu_\tau \bar{\nu}_\tau$	6.6 %	20 %
$e^+ e^-$, $\mu^+ \mu^-$ or $\tau^+ \tau^-$	3.3 %	10 %
$u\bar{u}$ or $c\bar{c}$	12 %	
$d\bar{d}$, $s\bar{s}$ or $b\bar{b}$	15 %	70 %

Table 2.5: Probabilities for the decay of Z^0 into possible primary fermions

2.2.4 Strong Interactions - QCD

After the Z^0 has decayed, the two primary quarks move apart in opposite directions. The further evolution from $q\bar{q}$ into the final state is described by *Quantum Chromo Dynamics* (QCD[5]), the theory of strong interactions.

In its basic concept it is a copy of QED, which means it is also a gauge theory. However, the underlying symmetry group is more complex and has properties which makes QCD very different from QED.

The QCD analogues to QED electric charge is color charge. Three types of color charges exist: red, green and blue. The symmetry group is the non-abelian group $SU(3)_C$. By requiring the QCD Lagrangian to be gauge invariant under a SU(3) transformation, $8(= 3^2 - 1)$ gauge fields need to be introduced. They are referred to as gluons, and since SU(3) is non abelian, quarks *and* gluons carry color charge.

The Lagrangian of QCD is

$$\mathcal{L}_{QCD} = \bar{q}(\imath\gamma^\mu \partial_\mu - m)q - g(\bar{q}\gamma^\mu T_a q)G_\mu^a - \frac{1}{4}G_{\mu\nu}^a G_a^{\mu\nu} \tag{2.34}$$

with g the coupling constant, T_a the generators of SU(3) and G_a the eight color fields (gluons). The last term stands for gluon self interaction. This becomes more clear if the Lagrangian is rewritten with

$$G_{\mu\nu}^a = \partial_\mu G_\nu^a - \partial_\nu G_\mu^a - g f_{abc} G_\mu^b G_\nu^c \tag{2.35}$$

in a more symbolic way (see figure 2.2)

$$\mathcal{L}_{QCD} = "\bar{q}q" + "G^2" + g"\bar{q}qG" + g"G^3" + g^2"G^4" \tag{2.36}$$

The first three terms, free quark/gluon propagation and quark-gluon interaction, have QED analogues. The three and four gluon vertex, however, are unique to QCD and reflect the fact that gluons themselves carry color charge.

This has a deep impact on the behavior of quarks and gluons. As long as the particles are close together (high Q^2), they hardly feel the strong force because the coupling constant α_S is small ($\alpha_s(Q^2 = M_Z^2) = 0.12$) and it is possible to compute color interactions using the perturbative techniques familiar from QED. At larger distances, however, α_S becomes bigger ($\alpha_s \approx 1$) and perturbation theory fails at all or becomes too complicated and elaborate for practical use. This behavior is called *asymptotic freedom* and *confinement*.

Due to the confinement it is not possible to observe a single quark/gluon. Only colorless formations of partons exist: mesons ($q\bar{q}$), baryons (qqq) and anti-baryons ($\bar{q}\bar{q}\bar{q}$).

To leading order, the dependence of α_S on the energy scale Q^2 of a process is

$$\alpha_S(Q^2) = \frac{12\pi}{(33 - 2n_f)\log(Q^2/\Lambda^2)} \tag{2.37}$$
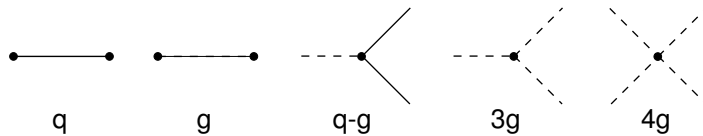
Figure 2.2: Schematic representation of the QCD Lagrangian

where n_f is the number of flavors possible. α_S is small as long as Q is big compared to Λ and gets large when Q is of the order of Λ. The parameter Λ can be seen as marking a boundary between quasi-free quarks/gluons and the world of hadrons. It is a free parameter of QCD and is determined by experiment. The value is about the inverse size of a typical hadron (≈ 0.2 GeV[1]).

The process of fragmentation is subdivided into these two stages, namely the perturbative region, where quarks and gluons are more or less free particles, and the non-perturbative region, where the strong force gets *really* strong and starts to bind the partons into colorless hadrons.

2.2.5 Fragmentation: Perturbative Region

The principle of perturbation theory is to express a physical quantity T (i.e. a solution to an equation which cannot be solved exactly) in terms of a power series in a small parameter. $\alpha_{e.m.}(M_Z^2) \simeq 1/128$ of QED is a good example. The (approximated) solution is then given by

$$T(\alpha) = T_0 + \alpha T_1 + \alpha^2 T_2 + ... \tag{2.38}$$

If α is small compared to unity the series might converge rapidly and already the first term only is a very good approximation of the real solution. If, however, α is of the order of 1 (or bigger) the series does not converge at all and a perturbative expansion of the solution is not possible.

Two methods are in use to simulate the perturbative region (see figure 2.1b) of the process $e^+e^- \to hadrons$:

(i) Matrix Element Method

This method[2] is based on exact calculations of feynman diagrams for all (possible) orders of perturbation theory. For first order calculations, in addition to the basic process $e^+e^- \to q\bar{q}$, one quark emits a gluon. Initially a $2 \to 3$, i.e. $e^+e^- \to q\bar{q}g$, process has 9 variables of which 5 are independent. After integration over the three Euler angles, 2 independent variables remain. One choice is the scaled energies of q and $\bar{q}$

$$x_q = \frac{E_q}{\sqrt{S}/2}$$
$$x_{\bar{q}} = \frac{E_{\bar{q}}}{\sqrt{S}/2} \tag{2.39}$$

The differential cross section for this process is

$$\frac{d^2\sigma}{dx_q dx_{\bar{q}}} = \sigma_0 \cdot \frac{C_F \alpha_S}{2\pi} \cdot \frac{x_q^2 + x_{\bar{q}}^2}{(1 - x_q)(1 - x_{\bar{q}})} \tag{2.40}$$
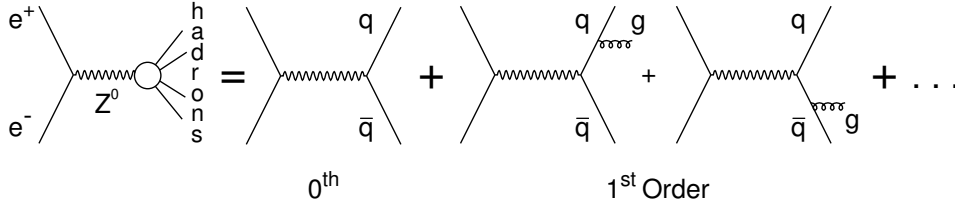
Figure 2.3: The physical vertex as a sum of the perturbative orders

with $C_F = 4/3$ (color factor) and

$$\sigma_0 = \frac{4\pi\alpha_S}{3S} \cdot N_C \cdot \sum_{d,u,s,\ldots} Q_f^2 \qquad (2.41)$$

For certain values of the kinematic variables $x_q, x_{\bar{q}}$ the cross section is divergent

(a) $x_q \to 1 \Rightarrow \bar{q}$ and g are collinear

(b) $x_q \to 1$ and $x_{\bar{q}} \to 1 \Rightarrow$ soft gluon radiation (q and $\bar{q}$ almost back-to-back)

These divergencies are of a non physical nature. They come from the fact that the physical vertex of this reaction is not only made up of the basic process (0th order) and first order, but is the sum of all orders of perturbation theory (see figure 2.3). In fact, interference terms of 2nd order feynman diagrams with 0th order give a contribution to 1st order and all divergencies of first order cancel out. This is called renormalization and is a very important aspect of the theory. For the total cross section of $e^+e^- \to hadrons$ in terms of a perturbation series in α_S one gets

$$\sigma = \sigma_0(1 + \frac{\alpha_S}{\pi} + \ldots) \qquad (2.42)$$

In general, it cannot be said if a matrix method calculation, which at present is possible up to $O(\alpha_S^2)$, is sufficient to reproduce data. At a center of mass energy of 91.2 GeV ($= M_Z$) it turns out that this is not the case and that another model has to be used.

(ii) Parton Shower Model

The parton shower model[2] is a different approach to simulate the perturbative region of fragmentation. It is simulated by a successive (independent) branching of partons, starting from the primary pair. The basic structure of the shower is made up by three branching processes: $q \to qg$, $g \to gg$ and $g \to q\bar{q}$. Each process is characterized by the so called Altarelli-Parisi splitting kernels

$$P_{q \to qg} = C_F \frac{1 + z^2}{1 - z}$$
$$P_{g \to gg} = C_A \left(\frac{z}{1-z} + \frac{1-z}{z} + z(1-z) \right)$$
$$P_{g \to q\bar{q}} = \frac{n_f}{2}(z^2 + (1 - z^2)) \qquad (2.43)$$
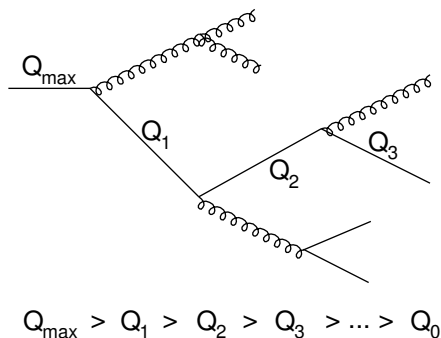
13

$$Q_{max} > Q_1 > Q_2 > Q_3 > ... > Q_0$$

Figure 2.4: Parton cascade

The branching rate is proportional to $\int P_{a \to bc}(z)dz$. The z value of the branching describes the energy sharing among daughter partons b and c. Parton b gets a fraction z of the mother energy, parton c gets $(1-z)$. The two daughter partons can then split again, and so on. With this approach, almost any order in α_S can be simulated. In addition to z, each parton is characterized by a virtuality scale Q^2, where the very first parton in the shower has a virtuality of Q_{max}. In final state showers, Q^2 decreases at each branching (see figure 2.4)

In PYTHIA, Q^2 is associated with m^2 of the branching parton. Starting from Q_{max}, the first parton evolves down in Q^2 until a branching occurs. The selected Q^2 defines the mass of the branching parton, and the z of the splitting kernel the energy sharing among the daughters. These daughters also evolve down in Q^2 separately, where their starting virtuality scale is given by kinematics. When Q reaches Q_0 the parton shower is stopped. From this point on perturbative calculations are no longer valid, due to the rise in α_S. In addition, corrections to the leading-log picture ($\to$ soft gluon interference) lead to an ordering of subsequent emissions in terms of decreasing angles. A detailed description of the parton shower model can be found in[2].

2.2.6 Fragmentation: Non-Perturbative Region

After the parton shower is stopped the set of colored partons needs to be evolved into the final observable colorless hadrons. Since the underlying physics, i.e. QCD in the strongly interacting region, is not yet completely understood, several phenomenological models have been developed. Three of them are widely used: string fragmentation, independent fragmentation and cluster fragmentation.

Only string fragmentation[2] will be discussed in a bit more detail since it is the default fragmentation model of the event generator PYTHIA used in this study.

The partons delivered by the parton shower are connected via a color field due to the strong force. To explain the basics, consider an initial parton configuration made up of two quarks only. The string stretches from quark to antiquark. Coulomb forces are neglected and the approximation is made that the energy in the string increases linearly with the separation of the two quarks. The amount of energy per unit length of the string is $1\frac{GeV}{fm}$. On further separation of the partons, energy increases and the string may break up into a new $q'\bar{q}'$ pair. One of the two new string pieces is assumed to be a hadron. The energy/momentum of it is calculated by probabilistic functions. Further breakups may occur if the invariant mass of the remaining string piece is large enough. In the Lund string model[9] implemented in PYTHIA,

breakups occur until only on-mass-shell hadrons remain.

In general, breaking of the string can be started at either side of it. Starting at q should give the same results as starting at $\bar{q}$. This symmetry is a constraint on the so called *Lund symmetric fragmentation function*, which has two free parameters a and b. They are determined from data (see section 7.3.1).

The treatment of a multi-parton configuration is complicated due to the number of string pieces moving in different directions and due to different possibilities to connect the partons. Calculable matrix elements of perturbative QCD contain interference terms between the possibilities and they are found to be down in magnitude by a factor $\frac{1}{N_C^2} = \frac{1}{9}$[2]. Hence, approximations with no interference terms can be found.

Meson production is directly understood by this breaking of strings into lower energy pieces. Baryons, however, are made up of three quarks and the simple picture of $q\bar{q}$ string pieces does not lead to three quark colorless hadron production. Different models for baryon production are used, an overview is given in [2].

After the energy of the string pieces is too low for further breakups the (almost) final state of the process of electron-positron annihilation into hadrons is reached. The last step is the decay of resonances into *stable* particles.

At the end of this section it should be said that nature does not distinguish between the two steps (b) and (c) of figure (2.1). To handle the problem by means of a perturbative and then a non-perturbative approach is a purely artificial separation of the whole process. The boundaries between the regions are not fixed, but given by model parameters (Λ_{QCD},Q_0) which need to be tuned to describe data. Many aspects of this process are yet not understood and therefore some observable effects are not reproduced by the simulation. The Bose-Einstein Effect, which is subject of this thesis, is a good example.

2.2.7 Decay of Short Lived Particles

The last step to the final state is the decay of short lived particles. Actually most of the particles of the *up to now* final state are unstable. Nevertheless, many of them can be treated as stable because they, on average, do not decay before they leave the detector. The definition of the lifetime above which a particle is considered stable has to be specified and is also influenced by the size of the detector. For a MC sample on hadron level of the simulation, all particles with a mean lifetime above 10^{-9} seconds are stable (e.g. $\pi^\pm$ or $K^\pm$). A π^+ with a mean lifetime of $\tau = 2.6 \cdot 10^{-8}$ seconds and a mean momentum of $\bar{p} = 3.37$ GeV, for example, on average travels a distance of 190 meters before it decays. This is far outside of the detector and therefore it is *stable*.

For a full detector simulation, however, all decays are taken into consideration because it is also possible that a π^+ decays inside the detector.

2.2.8 Charged Particle Composition of the Final State

To give an overview of the composition of charged particles in the final state a PYTHIA MC sample on hadron level ($N_{ev} = 2\cdot10^6$) was used. The mean charged multiplicity is $\langle n_{ch}\rangle = 20.66$. Table (2.6) shows the average numbers and average percentages of charged particles in the final state.

	$\pi^{\pm}$	$K^{\pm}$	$p^{\pm}$	$e^{\pm}$	$\mu^{\pm}$
$\langle n \rangle$	16.94	2.14	1.07	0.38	0.14
in %	82.0	10.4	5.4	1.8	0.68

Table 2.6: Average number of charged particles in the final state

On average, 82% of all charged particles in the final state are charged pions (either π^{+} or π^{-}). This makes the pion the most frequently produced charged particle of the hadronic final state. The main contribution to the measured Q-distribution (see chapter 5) will therefore come from pairs of pions.

Chapter 3

Experimental Setup

3.1 The ALEPH Detector

The basis of this study is data taken by the ALEPH collaboration in the year 1994. The ALEPH detector was one of four detectors which were built and used for the **L**arge **E**lectron **P**ositron collider (LEP) at the European Organization for Nuclear Research (CERN), Geneva. ALEPH itself is not only the first letter in the Hebrew alphabet, where the ALEPH logo א comes from, but also stands for **A**pparatus for **LEP** p**H**ysics. Figure $(3.1)^1$ shows a schematic sketch of the LEP accelerator. It has a circumference of about 27 km and is located approximately 100 meters underground. The electron and positron beams are injected, after being pre-accelerated in various smaller accelerators, in opposite directions and brought to an energy of 45.6 GeV ($=M_Z/2$) each. The two beams intersect at four different places around the ring, exactly were the four large detectors are situated.

The ALEPH detector itself is shown in figure $(3.2)^1$. It has a cylindrical shape with the beam pipe as its axis. The size is about $12 \times 12 \times 12$ m^3 and its weight about 3000 tons. The different sub-detectors like Time Projection Chamber (TPC) or Electromagnetic Calorimeter (ECAL) are arranged in cylindrical layers around the beam pipe with end caps on either side. In multihadronic Z decays, outgoing particles cover a solid angle of 4π and events have an average multiplicity of about 20 charged and 20 neutral particles. Therefore the detector was designed to have hermetic coverage and accurate vertexing.

For this study the momentum and 2-track resolution of the detector is important and will be discussed in a bit more detail in the next section. An overall description of the detector and its performance can be found elsewhere [10, 11].

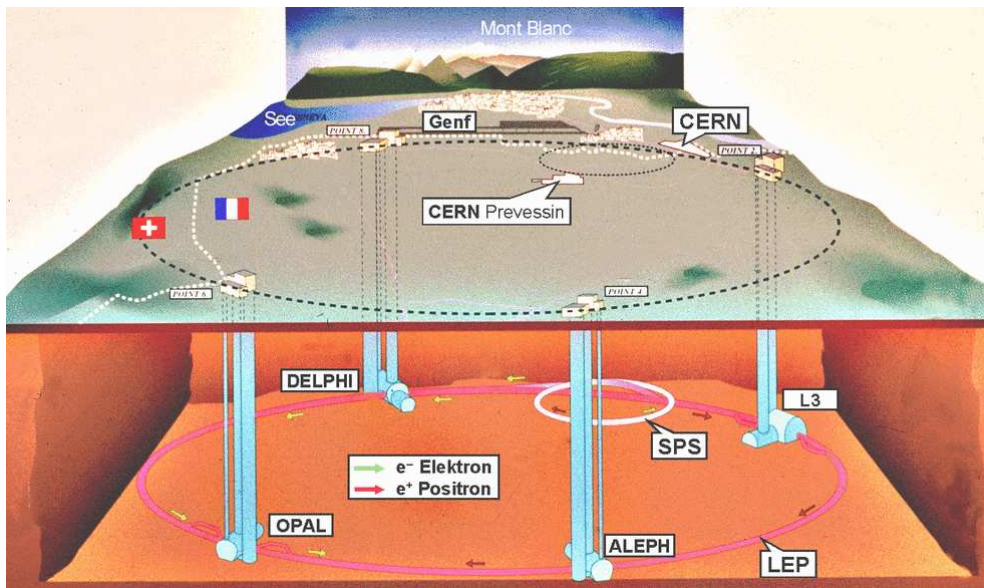[1] taken from the CERN photo database

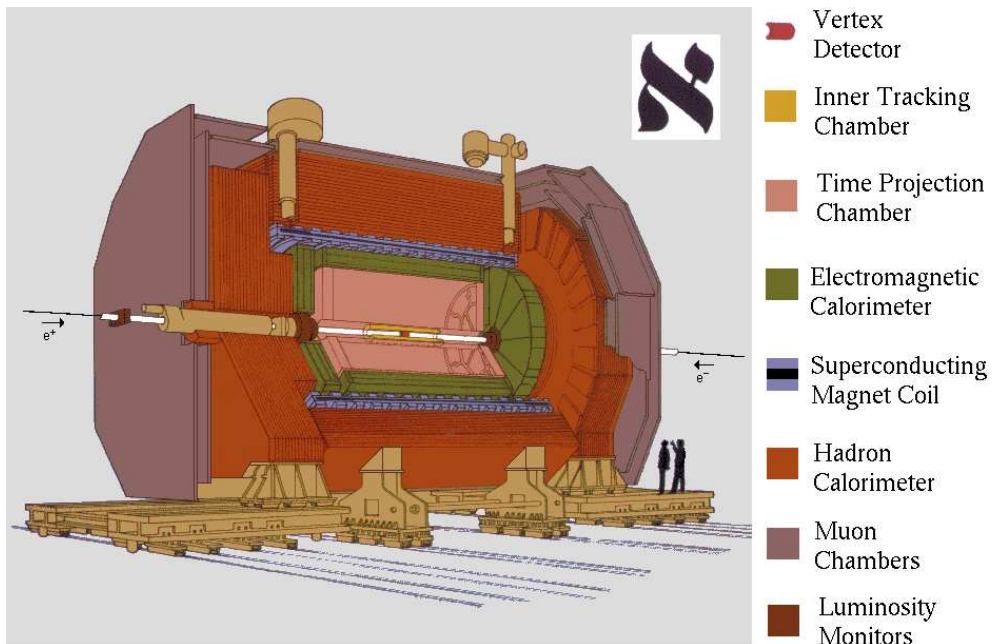Figure 3.1: The Large Electron Positron Collider at CERN

Figure 3.2: The ALEPH detector
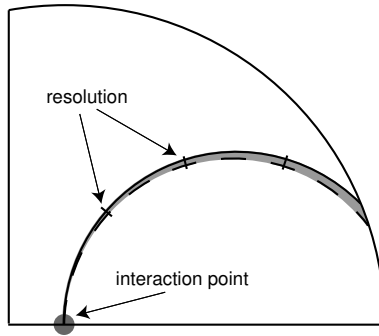
Figure 3.3: 2-track resolution

3.2 Momentum and 2-Track Resolution

The main quantity to be measured is the so called Q value of a pair of like-sign charged particles, and herein especially pairs with small Q values (Q < 0.5 GeV) are of interest. As presented later, only pairs close in phase space, i.e. $\vec{p}_i \approx \vec{p}_j$ and $E_i \approx E_j$, have a small Q value. Therefore it is important to have a very good momentum and/or energy resolution within the detector.

The momentum of a charged particle is determined in the three innermost detectors, namely the *silicon vertex detector* (VDET[13]), the *inner tracking chamber* (ITC[14]) and the *time projection chamber* (TPC[15]), by measuring the particles' curvature due to the magnetic field (1.5 T) in the inner detector. The momentum resolution is given by

$$\sigma(1/p_t) = 0.6 \times 10^{-3} (GeV/c)^{-1} \tag{3.1}$$

(at 45 GeV) where p_t is the transverse momentum[11]. With the 3 dimensional track information of the TPC, the angle between the beam axis and $\vec{p}$ (at the production point of the particle) is known and p_z can be calculated.

The energy of a particle is then $E^2 = \vec{p}^2 + m_\pi^2$, where $m_\pi \approx 140$ MeV is the pion mass, which is assumed for all charged particles.

The limited spatial resolution in the TPC (about 180 μm for rΦ and 0.8 mm for the z direction [12]) also leads to a limited 2-track resolution (see figure 3.3). The hits of the particles in the TPC and therefore their *real* tracks (continuous and dashed line) are very close together and are misidentified during reconstruction as being only one particle (shaded area). The overall track reconstruction inefficiency is reproduced by the simulation to better than 10^{-3}[16].

Chapter 4

Particle Correlations

4.1 BE-Statistics

Consider a region in space where particles are produced[17]. The amplitude for emission of a pion with momentum $\vec{p}_1$ from a point $\vec{x}_A$ is $e^{\imath \vec{p}_1 \cdot \vec{x}_A}$. If one could distinguish between two identical pions, the joint probability amplitude for the emission of two pions at points $\vec{x}_A$ and $\vec{x}_B$ would be

$$e^{\imath \vec{p}_1 \cdot \vec{x}_A} e^{\imath \vec{p}_2 \cdot \vec{x}_B} (e^{\imath \Phi_A} e^{\imath \Phi_B}) \tag{4.1}$$

with phases Φ_A and Φ_B. However, since the pions are indistinguishable particles, the amplitude must be made Bose symmetric, i.e. symmetric under particle exchange

$$A_{12} = \frac{1}{\sqrt{2}} (e^{\imath \Phi_A} e^{\imath \Phi_B}) \left[e^{\imath \vec{p}_1 \cdot \vec{x}_A} e^{\imath \vec{p}_2 \cdot \vec{x}_B} + e^{\imath \vec{p}_2 \cdot \vec{x}_A} e^{\imath \vec{p}_1 \cdot \vec{x}_B} \right] \tag{4.2}$$

The joint probability for two identical bosons is then

$$P_{12} = |A_{12}|^2 = 1 + \cos(\triangle \vec{p} \cdot \triangle \vec{x}) \tag{4.3}$$

with $\triangle \vec{x}$, $\triangle \vec{p}$ as the space and momentum difference of the two pions, respectively. Let the points of pion production be distributed with a function $\rho(\vec{x})$ and integrate (4.3) over $\vec{x}_A$ and $\vec{x}_B$, you get

$$P_{12} = 1 + |\tilde{\rho}(\triangle \vec{p})|^2 \tag{4.4}$$

$\tilde{\rho}$ is the normalized Fourier transform of ρ and tends to unity as $\triangle \vec{p} \to 0$. This means that for small values of $\triangle \vec{p}$ the production probability of two identical pions is enhanced. So far, equation (4.4) has two shortcomings:

- only valid for a completely chaotic source

- no time dependence

Both shortcomings can be addressed by introducing a new parameter λ and allow $\tilde{\rho}$ to be a function of the four vector $\triangle p$ instead of $\triangle \vec{p}$

$$P_{12} = 1 + \lambda |\tilde{\rho}(\triangle p)|^2 \tag{4.5}$$
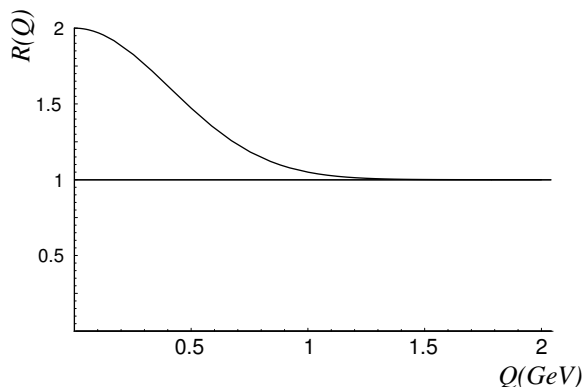
Figure 4.1: Enhanced pair production at low Q values

λ is a measure of coherence of the particle emitting source and takes the value 1 for a completely chaotic source and 0 for a completely coherent source. Therefore it is also referred to as a measure of strength of the BE effect.

To get a more meaningful expression for (4.5) we make the following assumptions about the source of particle production

- the particle emitting source is spherically symmetric

- the point of production is distributed with a gaussian of width σ

- the source is exponentially decaying with $e^{-\frac{t}{\tau}}$

The result is

$$R(Q) := P_{12} = 1 + \lambda e^{-\frac{Q^2}{\sigma^2}} \tag{4.6}$$

with

$$Q := \sqrt{-(p_1 - p_2)^2} \tag{4.7}$$

Again, for pairs of pions with a small Q value, i.e. pairs which are close in momentum space, the production probability P_{12} is enhanced (see Fig. 4.1). This is called *Bose-Einstein Effect.*

4.2 Q-Distribution

A sensitive observable to measure this effect is the so called Q distribution of identical bosons given by

$$\rho(Q) := \frac{1}{N_{ev}} \frac{dn}{dQ} \tag{4.8}$$

It is a measure of how many pairs lie within a certain Q interval dQ, normalized to the number of events N_{ev}. The theoretical prediction for the Q-distribution is now that due to the BE effect it should show an enhancement in number of pairs with a small Q value compared to what uncorrelated production would give.

A good way to study BE correlations is therefore to divide a measured or MC (with BE) generated Q-distribution bin-by-bin by an BE unaffected sample. For small Q values this ratio should be clearly above unity. Since it is impossible to measure distributions of identical bosons in the absence of BE, other types of reference samples have to be considered (see next section).

When the choice of reference sample has been made the following ratio is the observable of interest

$$C(Q) = \frac{1}{N_{Data}} \left(\frac{dn}{dQ} \right)_{Data} / \frac{1}{N_{MCnoBE}} \left(\frac{dn}{dQ} \right)_{MCnoBE} \qquad (4.9)$$

C(Q) is called correlation function. It is a measure of how the Q distribution is changed by BE. The choice of a parameterization of C(Q) is important when MC samples which include the simulation of BE effects need to be generated. A very basic form is given in (4.6). Due to theoretical considerations, various (more sophisticated) parameterizations are used and tested to implement BE correlations (see chapter 6).

4.3   Reference Samples and Resonance Decays

For this thesis a reference sample is only needed to *make the BE effect visible* by means of the correlation function (4.9). If one wants to determine parameters for a certain parameterization of this function, one has to be careful because the parameters depend on the reference sample used.

One choice is to take a Monte Carlo generated one with no simulation of BE implemented. This type of reference sample is used in this study. Another, but more delicate choice is to take a measured distribution from unlike-sign pairs (like $\pi^+\pi^-$) with the assumption that, due to the opposite charge, it is not affected by BE. It is shown, however, that BE correlations acting between identical pions may have significant indirect effects on distributions of non identical pions. This is called *residual BE effect*[18]. A second result of residual BE correlations in $\pi^+\pi^-$ is an apparent change in line shapes of certain resonance decays. An example is the decay of $\rho(770)^0$ into $\pi^+\pi^-$[18].

A third possible reference sample can be obtained by means of an event mixing technique. It is obvious that identical bosons of two different events do not interfere with each other. If the Q distribution is constructed with identical pairs, where one particle comes from the first event and the other from the second, it is possible to get a BE unaffected reference sample.

Chapter 5

Experimental Q-Distribution

5.1   Event Selection

For this study, ALEPH data containing 1 million hadronic Z-decays from 1994 were analyzed. The event selection of $q\bar{q}$ candidates is purely based on information about charged tracks in the final state. The so called CLAS 16 predefined ALEPH hadronic event selection was used, which is defined as follows[19]:

- the event has to contain at least 5 TPC tracks which have

  - more than 4 hits in the TPC
  - a radial distance to the beam axis $|d_0| < 2$ cm
  - a distance on the beam axis from the interaction point $|z_0| < 10$ cm
  - $|\cos\theta| < 0.95$, with $\theta = \measuredangle$ (beam axis to charged track)

- in addition, the energy sum of all TPC tracks satisfying the cuts above, should have more than 10% of the total center of mass energy $E_{cm} = 91.2$ GeV

With these cuts the selection efficiency for hadronic events is almost 100%. Only events which are well contained within the detector are selected by the cut $|\cos\theta(thrust-beam)| < \cos(30°)$. To reduce residual background events (mainly $e^+e^- \to \tau^+\tau^-$ and $\gamma\gamma$ reactions), which pass the CLAS 16 selection criteria, additional energy flow cuts are applied:

- $(\sum E_{ch+n})/E_{cm} > 0.5$

- N(energy flow objects) > 12

$\tau^+\tau^-$ background events are reduced to less than 0.3% of all selected events and are therefore negligible for most analyses[16].

For the experimental Q-distribution additional cuts for charged tracks were used. These are the type=0 tracks of the ENFLW energy flow algorithm[19].

- use only charged tracks which come from the interaction point

- reject $e^\pm$ with p > 1 GeV

- reject $\mu^\pm$ with p > 2 GeV

5.2 Experimental Evidence for BE

As stated earlier the Q-distribution of identical bosons should show an enhancement in production of pairs with a small Q value, i.e small 4-momentum difference. Figure (5.1a) shows
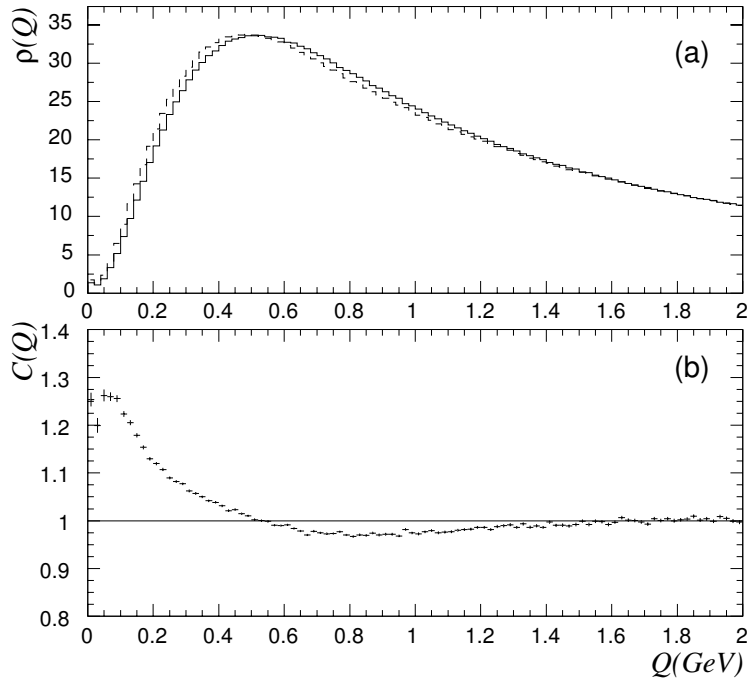
Figure 5.1: (a) measured (dashed line) and MC generated (continuous line) Q-distribution. (b) the ratio C(Q) (see 4.9) of the two distributions.

two Q-distributions. A measured one from 1994 LEP data taking (dashed line) and a MC generated one (1994) with no BE implemented (continuous line). The MC sample was further sent through a detector simulation to be comparable to the uncorrected data. The ratio C(Q) (see 4.9) of the two distributions is shown in (b). Towards smaller Q values a clear rise in C(Q) above unity can be seen. This is due to the Bose-Einstein effect.

A remark to the measured Q-distribution is that it actually is not known if two charged tracks are identical bosons. Therefore it happens that also the Q value of a non-identical pair (e.g. $\pi^+ K^+$) contributes to the overall Q-distribution. However, since more than 80% of all charged tracks (see section 2.2.8) are charged pions, their contribution to the Q-distribution is the largest.

Chapter 6

MC Event Generators and BE

6.1 Introduction

Monte Carlo event generators are widely used in physics, especially in high energy physics. The aim is to describe and reproduce many characteristics of a given physical process like $e^+e^- \rightarrow hadrons$ (see figure 2.1). The basis to simulate this process is theory presented in chapter 2, the *language* of the generator, however, is a probabilistic one. Everything is simulated by means of probabilistic expressions: splitting functions, flavor composition of initial quark pairs, branching ratios a.s.o. Event samples generated with these programs are in very good agreement with real measurements. Many model parameters (see next section) are used to control the event generator used and to simulate the physical processes which take place. A high accordance between data and simulation can only be accomplished if all the parameters are tuned to describe measured distributions as accurate as possible.

Nevertheless, due to the probabilistic treatment of physical processes some measured effects can not be described properly. The Bose-Einstein effect is a very good example.

When BE needs to be implemented into a MC event generator, a principal choice between two different approaches has to be made

- Implementation within the framework of event generation, i.e. simulation of the BE effect at some stage of the event generation process. This is the approach of PYBOEI, the BE simulation routine of PYTHIA[2].

- *Afterwards* implementation, i.e apply a BE simulating algorithm onto existing MC samples. This is the approach of a model proposed by V.Kartvelishvili and R.Kvatadze. Their model will be further denoted as K+K[21].

Both approaches have advantages and shortcomings which will be addressed in subsequent sections. Throughout this study (also for K+K), PYTHIA (Version 6.152) was used to generate events.

6.2 PYTHIA

PYTHIA is a very commonly used event generator in high energy physics. The program is capable of simulating e^+e^-, proton-proton and e^--proton collisions in a large energy range. Many different physical processes (about 240 hard processes like $qg \rightarrow qg$ for example) are included. Due to it's versatile applicability it offers a multitude of parameters and switches

to be used and varied. Only parameters/switches explicitly used/changed in this study for event generation are presented in table (6.1). All other parameters and switches have PYTHIA default values. BE related parameters and QCD parameters which are varied in this study are described in chapter 7.

PARJ(1)	0.108	suppression of diquark-antidiquark pair production compared with $q\bar{q}$ production $\rightarrow \mathcal{P}(qq)/\mathcal{P}(q)$
PARJ(2)	0.286	$\mathcal{P}(s)/\mathcal{P}(u)$
PARJ(3)	0.69	$\{\mathcal{P}(us)/\mathcal{P}(ud)\}/\{\mathcal{P}(s)/\mathcal{P}(d)\}$
PARJ(11)	0.553	probability that a light meson (with a u or d quark) has spin 1
PARJ(12)	0.470	probability that a strange meson has spin 1
PARJ(13)	0.65	prob. that a charmed or heavier meson has spin 1
PARJ(17)	0.20	prob. that a meson with spin 1, orbital angular momentum 1 and total spin 2 is produced
PARJ(26)	0.276	extra suppression factor for η' production
PARJ(42)	0.85	$b[\text{GeV}^{-2}]$ parameter for symmetric Lund fragmentation function
PARJ(54)	-0.04	ϵ_c
PARJ(55)	-0.002	ϵ_b
MSTJ(11)	3	choice of longitudinal fragmentation function 3 = hybrid fragmentation scheme
MSTJ(46)	0	azimuthal isotropy

Table 6.1: Overview of PYTHIA parameters and switches changed

6.3 PYBOEI - BE Simulation in PYTHIA

PYTHIA has a built-in routine for simulating BE effects called PYBOEI. It needs to be said that this routine is turned off by default. So most studies which use PYTHIA are carried out with no consideration of possible influences of BECs on the obtained results. It also underlines the fact that the provided implementations are far from being perfect. Even the authors of PYTHIA call it *a crude option for the simulation of Bose-Einstein effects*[2].

Nevertheless it is better to start somewhere than not to start at all. In the subsequent sections the general method, parameters, switches and variations of PYBOEI will be described and presented.

6.3.1 General Method of PYBOEI

In PYBOEI the simulation of BE effects is done within the framework of event generation. Fragmentation is allowed to proceed as usual and so is the decay of short lived particles. After their decay the simulation of Bose-Einstein effect starts and then long lived particles are allowed to decay, the evolution to the final state proceeds. The terms *short* and *long lived* are not to be

mixed up with the meanings given in section (2.2.7). Here, the meaning short/long is relative to the scale of hadronic interactions (see 6.3.4).

As mentioned earlier, BECs are supposed to enhance production of identical particle pairs with small Q values, i.e. which are close in momentum space. In terms of simulating BECs an increase in particle pairs with small momentum difference can be accomplished by shifting the momentum of identical pairs towards each other. This is the basic principle behind PYBOEI.

The procedure is as follows: A pair of identical particles is considered, e.g. $\pi^-\pi^-$, and it's Q value calculated

$$Q_{ij} := \sqrt{-(p_1 - p_2)^2} = \sqrt{M_{ij}^2 - 4m^2} \tag{6.1}$$

where M_{ij} is the invariant mass of the pair and m the common particle mass. The shift towards smaller Q values is done with the aim that the ratio (4.9) takes the form of a function f(Q) which parameterizes the BE effect (see chapter 4). A very basic parameterization is

$$f_2(Q) = 1 + \lambda e^{-(QR)^m} \tag{6.2}$$

with m = 1,2 , i.e. exponential or gaussian parameterization, respectively. If the inclusive distribution of Q_{ij} values is assumed to be given just by phase space (for small relative momentum), then, with $\frac{d^3p}{E} \propto \frac{Q^2 dQ}{\sqrt{Q^2+4m^2}}$, the shifted Q'_{ij} value can be found as the solution of

$$\int_0^{Q_{ij}} \frac{Q^2 dQ}{\sqrt{Q^2 + 4m^2}} = \int_0^{Q'_{ij}} f_2(Q) \frac{Q^2 dQ}{\sqrt{Q^2 + 4m^2}} \tag{6.3}$$

If Q'_{ij} is determined, its translation into a change of the 4-vector p_i of the particle i is not unique. Here the choice is made that the momentum of the pair (i, j) shall be conserved. The momentum shift of a particle i due to an identical particle j is $\delta\mathbf{p}_i^j$. It can be calculated by use of (6.1) and momentum conservation among the two particles, i.e. $\delta\mathbf{p}_j^i = -\delta\mathbf{p}_i^j$.

For our basic parameterization (6.2) only shifts to smaller momentum differences occur. For a parameterization which is not always above unity, Q'_{ij} can also be larger than Q_{ij}. The result is a shift of the two particles apart from each other. In general, functions will be used which, for intermediate values of Q, also dip a bit below unity.

All shifts are calculated with respect to the original momenta of the particles and then at the end each momentum is shifted. It is clear, that using this procedure, conservation of the total momentum of the event is granted. However, this so called local approach has other serious shortcomings.

By shifting momenta towards or apart, energy conservation is obviously fulfilled neither pairwise (locally) nor for the full event (globally). A possible solution is to re-scale all particle momenta in the rest frame of the event to restore energy conservation. This so called *global re-scaling* is purely ad-hoc and on the one hand does minimal harm for the study of a single Z-decay, but on the other hand, this must not hold for a pair of resonances. Other studies indeed show, that this kind of re-scaling introduces an artificial large shift in the reconstruction of the W mass in the process $e^+e^- \to W^+W^- \to hadrons$[22].

Therefore alternative methods to restore energy conservation have been considered, namely BE_{32}, BE_m and BE_λ.

The global energy re-scaling procedure of the basic algorithm is running counter to PYTHIA's philosophy that BECs should be local in nature. Energy should be conserved locally, and not by assigning one factor to the whole event. This, in general, is accomplished by calculating an

additional shift δr_k^l for a, not necessarily identical, pair of particles k and l. The final shift to ones particle momentum is then

$$\mathbf{p}_i' = \mathbf{p}_i + \sum_{j \neq i} \delta \mathbf{p}_i^j + \alpha \sum_{k \neq i} \delta \mathbf{r}_i^k \tag{6.4}$$

The α parameter is adjusted separately for each event so that the total energy is conserved.

6.3.2 BE$_3$ and BE$_{32}$

The very basic parameterization (6.2) was obtained by integrating (4.5) over a gaussian source. If, theoretically, a non-gaussian source of particle production is assumed, $f_2(Q)$ should show an oscillatory behavior, i.e. should go below unity as well. As indicated by data and by global model studies, the oscillations dampen out very quickly and for a simpler simulation it is accurate enough to use the first peak and dip only. The basic weight is therefore multiplied by a factor

$$\left(1 + \alpha\lambda \exp(-\frac{Q^m R^m}{3^m})\right) \tag{6.5}$$

and gets

$$f_2(Q) = \{1 + \lambda \exp(-Q^m R^m)\} \left\{1 + \alpha\lambda \exp(-\frac{Q^m R^m}{3^m})\right\} \tag{6.6}$$

which (with $\alpha < 0$) leads to values of $f_2(Q)$ smaller than unity. m=1(2), for exponential(gaussian) parameterization.

This parameterization is called BE$_3$ due to the 3^m in the denominator of the exponential. The factor is consistent with data but should not be given any deeper meaning. In this algorithm only identical particles are shifted additionally by δr_i^j. The shift is calculated like δp_i^j but by using the BE$_3$ weight (6.6) in (6.3). After these shifts are calculated, they are scaled by a factor α to restore energy conservation of the whole event. As expected α is negative, which means that some pairs are shifted apart.

It is, however, not the final weight because $f_2(0) \neq 2$ for $\lambda = 1$ as expected from theory. Another factor needs to be introduced

$$\left(1 - \exp(-\frac{Q^2 R^2}{2^2})\right) \tag{6.7}$$

and the final parameterization is then

$$f_2(Q) = \{1 + \lambda \exp(-Q^m R^m)\}$$

$$\times \left\{1 + \alpha\lambda \exp(-\frac{Q^m R^m}{3^m})\left(1 - \exp(-\frac{Q^2 R^2}{2^2})\right)\right\} \tag{6.8}$$

Due to the 3^m and 2^m in the denominator of the exponentials this method is called BE$_{32}$. We see that if $\lambda = 1$, $f_2(0)$ gets

$$f_2(0) = 1 + \lambda = 2 \tag{6.9}$$

as predicted by theory.

This weight can be viewed as a gaussian, smeared out representation of the first dip of the cosine function. The calculation for δr_i^j is done as for BE$_3$ and also with the BE$_3$ parameterization. Finally δr_i^j is scaled down by (6.7). The average value for α needed to restore energy conservation tends to be about -0.25.

This method is a mixture of a global and local approach to restore energy conservation. The momenta of the BE affected pair is shifted additionally by δr_i^j ($\rightarrow$ local) and the value of α has to be adjusted event by event ($\rightarrow$ global). Only then energy is conserved.

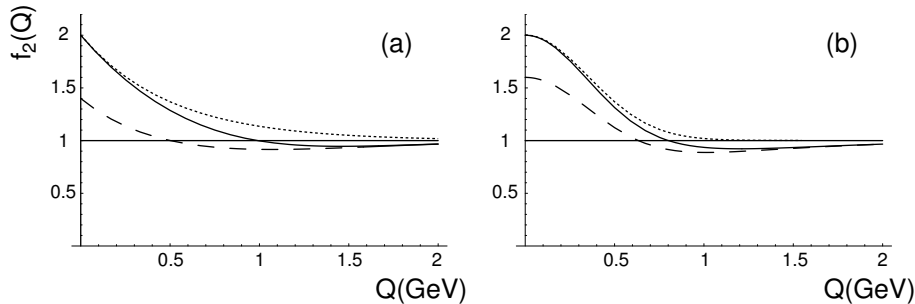Figure (6.1) shows f$_2$(Q) for BE$_3$ and BE$_{32}$ and the two possibilities of an exponential or gaussian basic weight.

Figure 6.1: The BE parameterization function f$_2$(Q) for BE$_3$ and BE$_{32}$

(a) Exponential parameterization for BE$_{32}$ (cont. line) and BE$_3$ (dashed line). For BE$_3$ it can be clearly seen that f$_2$(0) $\neq$ 2. The dotted line shows the exponential basic weight (6.2).

(b) Gaussian parameterization for BE$_{32}$ (cont. line) and BE$_3$ (dashed line). Again f$_2$(0) $\neq$ 2 for the BE$_3$ algorithm. The dotted line shows the gaussian basic weight (6.2).

6.3.3   BE$_m$ and BE$_\lambda$

For these two methods the original basic gaussian/exponential form of the parameterization function (6.2) is retained. These two are, other than BE$_{32}$ and BE$_3$, purely local methods. Energy is conserved by taking two particles in the vicinity of the identical ones and by shifting the momenta of these two particles apart. It is important to say that the two particles (k, l) may not be identical to each other nor to the BE affected pair (i, j). In detail, for each BE caused shift δp_i^j a corresponding δr_k^l of two close particles is found so that energy is conserved locally in the system of the four particles (i, j, k, l).

A principle problem of this method is how to define *closeness of particles*. A possible measure is that of a small invariant mass m_{ijkl} of the four particle system. So for a pair (i, j) two additional particles (k, l) are found with m_{ijkl}^{-2} being a maximum. In finding such two particles one has to be careful and aware of the following situation (see figure 6.2):

One of the two non-identical particles (say k) of the four considered *closest* has an identical partner nearby. The momentum shift required to produce a significant BE effect between k and its partner k' is small. Therefore, even though the final shift of each particle is applied only after all shifts are calculated, the shift of particle k due to energy conservation in the $ijkl$ system smears out the small BE caused shift due to k and its identical partner. It is therefore necessary to disfavor momentum compensation shifts that break up close identical pairs.
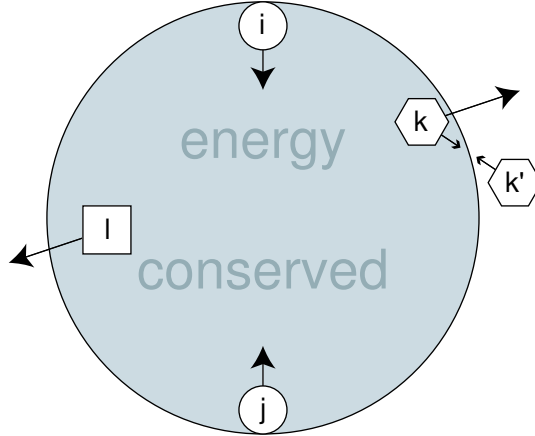
Figure 6.2: Breaking up of an identical pair due to energy conservation shift

In both algorithms, BE_m and BE_λ, a suppression factor for each of the two non-identical bosons (k, l) is defined as

$$\left(1 - \exp(-Q_k^2 R^2)\right) \cdot \left(1 - \exp(-Q_l^2 R^2)\right) \tag{6.10}$$

where Q_k and Q_l are the Q values to their closest identical partners.

In BE_m two particles (k, l) are chosen which maximize the measure

$$W_{ijkl} = \frac{\left(1 - \exp(-Q_k^2 R^2)\right)\left(1 - \exp(-Q_l^2 R^2)\right)}{m_{ijkl}^2} \tag{6.11}$$

If, hypothetically, k has an identical partner with $Q_k = 0$ the suppression factor is zero and W_{ijkl} is zero as well. Therefore it is not enough for a system $(ijkl)$ to have a small invariant mass m_{ijkl}. It is also necessary that no identical particles to k or l are close. It needs to be said however, that since two other particles have to be found to restore energy conservation, it is still possible (with reduced probability) that a close identical pair is broken up.

The algorithm denoted as BE_λ uses a different measure of closeness but again with the suppression factor (6.10). The so called λ measure (which is not the λ value that governs the strength of BE) corresponds to a string length in the Lund string model. It can be shown that hadrons close to each other have a small λ value, although with rather big fluctuations. The following measure

$$W_{ijkl} = \frac{\left(1 - \exp(-Q_k^2 R^2)\right)\left(1 - \exp(-Q_l^2 R^2)\right)}{min_{(12 permutations)}(m_{ij} m_{jk} m_{kl}, ...)} \tag{6.12}$$

is maximized. The denominator corresponds to $\exp(\lambda)$. Hence, if four particles are close, λ is small and W_{ijkl} gets big. If, however, identical particles to either k or l are nearby, W_{ijkl} is reduced again and some other particle has to be considered for energy conservation.

Since the invariant mass of many 4-particle systems, and every time the Q values of identical particles to (k, l) have to be calculated to figure out which system has the biggest value of W_{ijkl}, these last two methods are way more time consuming for computation (about a factor of 3 to 4) than BE_3 or BE_{32}.

6.3.4 Parameters and Switches

PYTHIA offers several parameters and switches to influence the behavior of PYBOEI, to chose between the different methods described above and to adjust the values used for parameterization. Table (6.2) and (6.3) show BE related parameters and switches which were used.

PARJ(92)	1.	λ_{BE}, strength of the BE effect
PARJ(93)	0.20 GeV	σ_{BE}, size of the BE effect region in terms of Q. The radius R_{BE} of the production volume is given by $R_{BE} = \hbar/\sigma \approx (0.2 fm \cdot GeV)/\sigma$
PARJ(91)	0.020 GeV	minimum resonance particle decay width

Table 6.2: BE related parameters of PYBOEI

MSTJ(51)	0	BE simulation off (default in PYTHIA)
	1	on, exponential parameterization
	2	on, gaussian parameterization
MSTJ(52)		particle classes involved in BE (1-9)
	3	π^+, π^- and π^0
	7	Pions and K^+, K^-, K_S^0, K_L^0
	9	Pions, Kaons and η, $\eta\prime$
MSTJ(54)		type of energy compensation
	0	BE_0
	1	BE_3
	2	BE_{32}
	-1	BE_m
	-2	BE_λ

Table 6.3: BE related switches of PYBOEI

In this study exponential and gaussian weight distributions were used. MSTJ(54) was set to 2, -1 and -2 and for these algorithms MSTJ(52) was set to 9, which means that all (MC-)possible bosons participate in BE. The values shown for PARJ(92) and PARJ(93) are PYTHIA default values for which a tuning was done (see chapter 7).

The parameter PARJ(91) needs to be discussed in more detail. As mentioned before, PY-BOEI implements BE effects after hadron resonances have decayed. The term *short lived* has

to be specified of course. A value of PARJ(91) = 20 MeV means that decay products (i.e. one of the 9 BE participating bosons) of resonances with a decay width of at least 20 MeV are considered *BEable* and their momenta are shifted according to the used algorithm. This, for example, includes decay products of ρ^0 and K^* (like $\rho^0 \to \pi^+\pi^-$ or $K^* \to K\pi$) but excludes particles which come from ω decays (e.g. $\omega \to \pi^+\pi^-\pi^0$).

Particles with a smaller decay width travel too far and their decay products are too far away from the production region to contribute to the BE effect. In terms of a mean lifetime only decay products of particles with $\tau < 3.3 \cdot 10^{-23}$ seconds are considered BEable.

6.4 Global Event Weight by K+K

An alternative approach to implement BECs into MC simulations is by use of a so called *global event weighting* procedure. A theoretical motivation for a possible global weight was given by B. Andersson and M. Ringner in [9]. In this study, a MC program written by V.Kartvelishvili and R.Kvatadze[21] was tested. Motivated by the shortcomings of PYBOEI, especially the necessary re-tuning of QCD parameters and the problems with local/global energy conservation, K+K tried to implement the ideas of Andersson and Ringner in a BE simulating algorithm. The theoretical motivation of this model is based on the fact that in the simulation of the hadronization process with PYTHIA, interference terms between different amplitudes of final states of identical bosons are not included. This lack might be responsible that BECs are not reproduced by PYTHIA (which if used with default values, runs without PYBOEI). Therefore, this model tries to include those terms with hindsight by calculating weights which are supposed to make up for the interference terms. Since this approach assigns a weight to an event as a whole, it is also called a global event weighting method. A further advantage is that no momenta are shifted, hence, energy is conserved by default.

6.4.1 General Method

Almost any hadronic final state contains, among other particles, a certain amount, say n, of identical bosons. If M is considered the matrix element describing the production of a hadronic final state, it needs to account for the $n!$ possible (undistinguishable) permutations P of identical bosons

$$M = \sum_P M_P \tag{6.13}$$

The matrix element of the simulation considers all possible permutations, however, does not include interference terms. The probability of the process, given by $|M|^2$, is therefore incomplete

$$|M|^2_{MC} = \sum_P |M_P|^2 \neq |\sum_P M_P|^2 = |M|^2 \tag{6.14}$$

It is shown that interference terms can be taken into account by assigning a weight to each event such that

$$|M|^2 = \sum_P \omega_P |M_P|^2 \tag{6.15}$$

and ω_P is given by

$$\omega_P = 1 + \sum_{P' \neq P} \frac{2\Re(M_P M_{P'}^*)}{|M_P|^2 + |M_{P'}|^2} \tag{6.16}$$

To be used in a simulation, M_P has to be parameterized. This is done with consideration of the Lund string model[9]

$$M_P = \exp[(\imath\kappa - \frac{b}{2})A_P]$$ (6.17)

where κ is the tension of the string (phenomenologically $\kappa \approx 1$ GeV/fm), A_P is the area of the breakup region of this particular boson configuration P and b describes the breaking probability of the string. With this M_P substituted into (6.16) we get

$$\omega_P = 1 + \sum_{P' \neq P} \frac{\cos(\kappa\Delta A_{PP'})}{\cosh(\frac{b}{2}\Delta A_{PP'})}$$ (6.18)

with $\Delta A_{PP'} = A_P - A_{P'}$.

This rather abstract parameterization can be linked to the parameters R and Q usually chosen to describe BECs. The product $\kappa\Delta A_{PP'}$ is estimated as an average BE interaction radius R times Q. The Q variable used in this approach coincides with the one used in PYBOEI (i.e. 4.7). The meaning of it is a somewhat different one and characterizes the difference in kinematics between the two permutations P and P'. The argument of the hyperbolic cosine in the denominator is also replaced by R · Q but multiplied by a model parameter ξ which needs to be adjusted phenomenologically.

With these replacements the weight gets

$$\omega_P = 1 + \sum_{P' \neq P} \frac{\cos(RQ)}{\cosh(\xi RQ)}$$ (6.19)

and, e.g. for only two identical bosons

$$\omega_2 = 1 + \frac{\cos(RQ_{12})}{\cosh(\xi RQ_{12})}$$ (6.20)

The important and new feature about this event weighting method is that the weight (6.19) goes slightly below unity for some intermediate values of Q (similar to (6.8)). This faces the problem of too large event weights of earlier approaches, because the total weight of an event is made up of the product of weights like (6.19).

With this parameterization the whole process of simulating BECs can in principle be applied on existing MC samples. The Q values for identical bosons and therefore the weight can be calculated with (6.19). The same 9 bosons as in PYTHIA are considered, namely π^+, π^-, π^0, K^+, K^-, K^0_S, K^0_L, η and $\eta\prime$, and the final weight is the product of the 9. The various event distributions (e.g sphericity, initial $q\bar{q}$ flavor, Q-distribution a.s.o.) are calculated as usual but afterwards multiplied by the obtained event weight.

From a computational point of view, this straight forward procedure is unfortunately not quite possible. Consider an event which has only 2 π^0's and 3 K^0_L's and no more than one of the other 7 types in the final state. The full event weight is (schematically) calculated as follows

$$\omega_{2\pi^0} = 1 + (12)$$
$$\omega_{3K^0_L} = 1 + (12) + (13) + (23) + 2 \times (123)$$
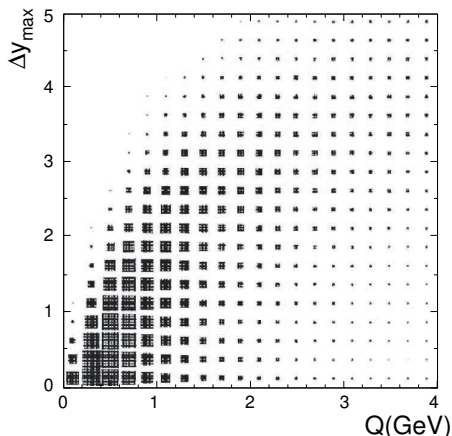$$\omega_{Event} = \omega_{2\pi^0} \cdot \omega_{3K^0_L}$$ (6.21)

Figure 6.3: Maximum rapidity difference Δy_{max} vs. Q

where e.g. (23) stands for $\cos(RQ_{23})/\cosh(\xi RQ_{23})$ and (123) for a circular permutation of all three K_L^0. This still looks quite manageable, but the final hadronic state of a Z^0 decay can have up to around 15 identical bosons of a kind. The number of permutation goes with $n!$, which means that for only one event and only one boson type, as a worst case scenario, $15! \approx 1.3 \cdot 10^{12}$ weights have to be calculated and summed! Together with 2 million events needed for proper statistics, it is obvious that the number of permutations has to be reduced. This can be accomplished by making good assumptions about which particles participate in BE and which don't.

6.4.2 Methods of Computation

Since BE effects are supposed to take place at some stage during the process of hadronization, decay products of long lived particles do not participate in BE. So similar to the lifetime cut ($\Gamma > 20MeV$) in PYBOEI a *distance of flight* cut is introduced. Decay products of a parent particle, which, in total (i.e including the distances its parents flew) travelled more than a cut off distance d_{max} before decaying, are not considered for BE. The value of d_{max} ranges between 10 and 80 fm and, when chosen, remains fixed throughout all events. After this cut with $d_{max} = 10$ fm about 42% of all π^+ remain, $\approx 58\%$ for $d_{max} = 40$ fm and $\approx 64\%$ for $d_{max} = 80$ fm. In contrary to the life time cut Γ of PYBOEI, d_{max} is not a lorentz invariant quantity.

Further on, not all permutations contribute to the summed weight (6.19). Mostly, the kinematic difference of two permutations P and P' is rather big and, hence, their contribution to BE small. It is therefore desirable to select permutations which are close in phase space to each other, i.e. which have a small Q value. However, calculating Q values for all possible permutations to filter out those with small ones brings us back to the start. It is better to do the following:

- calculate the rapidity of all bosons of a kind, given by $y = (1/2)\ln(\frac{E+p_z}{E-p_z})$, with respect to the thrust axis of the event
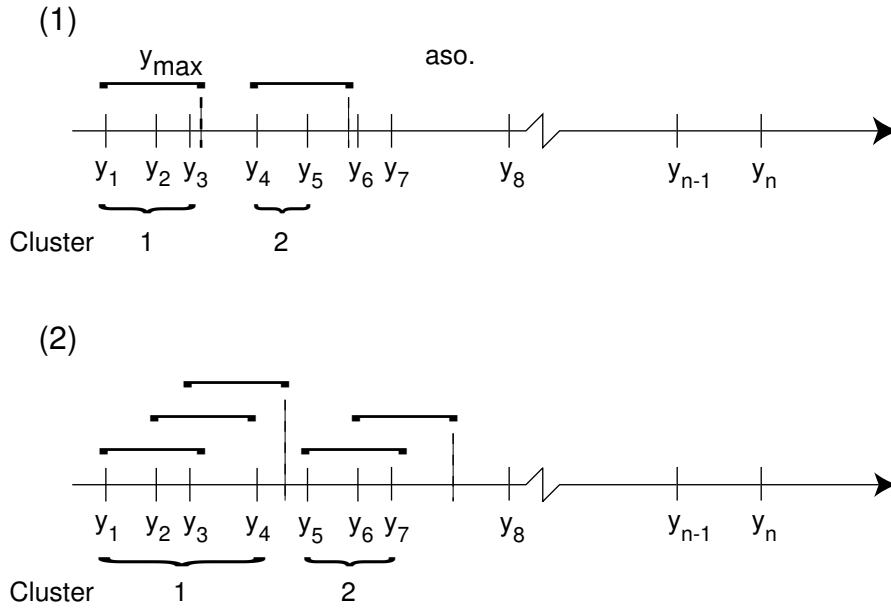
- order the particles according to their rapidity

(1)

(2)

Figure 6.4: Cluster methods used in K+K to reduce the possible number of permutations of identical bosons

- build clusters of up to n_{max} identical particles which have a maximum rapidity difference of less than Δy_{max} and calculate the weight for each cluster separately

- the overall weight for one particle type is given by the product of the cluster weights

A strong correlation exists between the largest difference in rapidity of a cluster and its Q values (see figure 6.3)[1]. This means that if only clusters with a Δy smaller than a certain Δy_{max} are considered, contributions with big Q are filtered out to a certain extend. But, more important, clusters with small Q (= big BE contribution) are kept, because there's almost no cluster with a y bigger than 1.5 and a Q smaller than 0.5 GeV.

Two different types of cluster algorithms have been used (see figures 6.4 and 6.5). The first method builds clusters with particles which have a $\Delta y < \Delta y_{max}$ with respect to the first particle. The second builds clusters with particles which have a $\Delta y < \Delta y_{max}$ with respect to the previous particle in the row. Method 1 (continuous line) prefers clusters with only one (no BE contribution) or two particles whereas method 2 (dashed line) has, as expected, an almost equal amount of one particle clusters but a tendency towards clusters with 3 or 4 particles (more than 4 particles are not allowed, see next section). Due to the looser clustering of method 2 there are more events which at least contain one cluster (i.e. with 2 or more particles), however, events with smaller and tighter clusters (smaller Q between the permutations) should contribute more to the overall weight than the bigger and looser cluster of method 2. Anyway, a clear prediction about which method will describe BE better cannot be made and we will see that simulation shows that there is not much difference between the results of both.
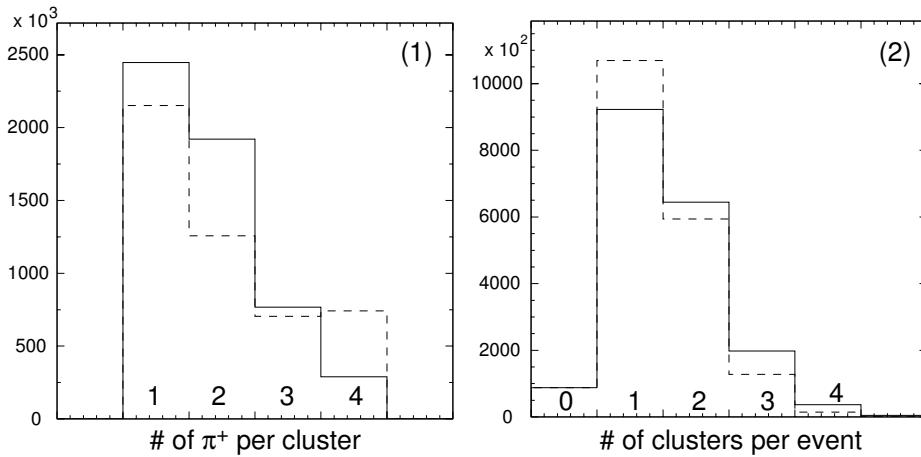
---

[1]taken from [21]

Figure 6.5: Comparison of the two cluster methods for π^+ with the respect to cluster size and number of clusters per event

6.4.3 Parameters

Due to the scheme of computation introduced the model has more parameters than would be necessary physically. Table (6.4) gives an overview of parameters and their values.

R	d_{max}	n_{max}	Δy_{max}
0.667 and 0.9 fm	10, 40, 80 fm	4	$6/n_{BEable}$

Table 6.4: BE related parameters of K+K

R and d_{max} have been described before. n_{max} is the maximum number of particles a cluster can contain and is chosen to be 4, which is a good compromise between computing time and strength of BECs, since bigger clusters are assumed to contribute less to BE. The maximum difference in rapidity of a cluster depends on n_{BEable}, i.e. the number of BEable particles of a kind in the event. If there are more particles, Δy_{max} is smaller and more tighter clusters, which are supposed to contribute more to BE, are formed. On average, for π^+ and $d_{max} = 40$ fm, there are between 4 and 6 particles per event. This means a $\Delta y_{max} \approx 1.$ - 1.5, which is rather harmless (see figure (6.3)).

For the basic noBE MC sample needed to apply the BE simulating algorithm, PYTHIA with the following values of QCD parameters was used. They were obtained by a tuning of noBE MC samples to existing data[20].

PARJ(81)	0.295 GeV	Λ_{QCD}
PARJ(82)	1.39 GeV	Q_0
PARJ(21)	0.366 GeV	σ, width of the gaussian p_x and p_y transverse momentum distributions for primary hadrons
PARJ(41)	0.40	parameter a of the symmetric Lund fragmentation function
PARJ(42)	0.885	parameter b of the symmetric Lund fragmentation function

Table 6.5: noBE best values for hadronization parameters

6.5 PYBOEI vs. K+K

Even though both methods described above have the same goal, i.e. the implementation of BECs into MC simulations, the way to accomplish it is quite different. It cannot be said in advance which way is best or which way will describe data better. Both have shortcomings and advantages and both can be as far and close to reality as can be imagined.

The physical idea behind the methods is very much the same and comes from the theory of particle correlations: it is assumed that BECs should enhance particle configurations of identical bosons which are close to each other.

One obvious difference in the strategy of achieving this aim is the treatment of BE as either local ($\rightarrow$ PYBOEI) or global ($\rightarrow$ K+K) in the sense that ...

... PYBOEI takes a pair of particles and shifts their momenta away or towards each other according to their Q value. Other particles in the event are not affected by this local shift, but treated separately - hence, BE is introduced as a local effect on close identical particles.

... K+K takes a look at the Q values of clusters of up to 4 identical particles and calculates a weight for the whole event. BE is then introduced as a common factor by which all calculated distributions have to be multiplied - hence, BE affects the event as a whole.

A small difference herein is that PYBOEI only takes pairs of particles into account, whereas K+K also uses clusters of up to 4 particles. As a consequence PYBOEI might overestimate the BE effect of 3 or more close identical particles by looking at them pairwise.

A further problem is that of the factorization property of QCD, which says that in the process of hadronization no influence on earlier stages of event evolution is possible. In other words, BE may not change initial quark flavor distributions, which are already given at parton level before BE takes place. As a consequence of an event weighting model, parton distributions also have to be multiplied by the event weight. This, however, as we will see later, can change parton distributions and thus the factorization property of QCD is not guaranteed.

A similar crucial issue is that of multiplicity: Does BE change the average number of particles produced in high energy physics experiments?

The answer is unknown. PYBOEI leaves the total multiplicity unchanged by definition, because shifting momenta does not produce new particles. K+K changes multiplicity of single events because the event weight has to be applied to the multiplicity distribution as well. The

intention of leaving average quantities unchanged by adjusting the average event weight $\langle \omega \rangle$ to 1 does not guarantee that this is true. And, see section 7.4.3, it is in general not the case.

In the next chapter both methods are used to simulate BE. The tuning procedure for BE and QCD parameters of PYTHIA as well as the application of K+K onto noBE MC samples is described and results are presented.

Chapter 7

Adjustment of Monte Carlo to Data

7.1   Correcting Data with Monte Carlo

Before a measured quantity can be compared with the results of other measurements or with theoretical predictions, it first needs to be corrected for detector related effects like geometrical acceptance, reconstruction efficiency or particle interactions with the material of the detector. Usually this is accomplished by multiplying the measured quantity $X_{measured}$ by a correction factor C

$$X_{corr} = C \cdot X_{measured} \tag{7.1}$$

Mostly the measured quantity is displayed in a frequency distribution also called histogram. The distribution is multiplied bin-by-bin by a correction factor which is calculated for this distribution only and for each bin separately. $X_{measured}$ could be, for example, one bin of the Q-distribution of like-sign charged particles.

The computation of the correction factor(s) has to be done for different studies individually. For the study of ALEPH hadronic events the following correction procedure was used[16].

Two MC samples have to be generated. The first one is designed to be as close as possible to what real events look like in the detector. They are generated including initial state radiation. These events are then sent through a detector simulation. For the ALEPH detector this program is called GALEPH[26]. The outcome is a MC sample on detector level which, for further analysis, can be treated just like real data. Fortunately, within the ALEPH collaboration, a large number of Jetset MC events is already available.

The second one is a well defined sample of what is expected to be seen in a perfect detector. No initial state radiation takes place and all final particles with a mean lifetime of more than 10^{-9} seconds are considered stable because they do, on average, not decay before they leave the detector. This includes particles like $\pi^{\pm}$ and K_L but not π^0, K_S, η or η'. In this way, only particles are in the MC final state which would also be seen for a real event in the detector. The outcome is a MC sample on hadron level. Both samples are produced using the same values for QCD parameters.

With these two samples the two corresponding quantities $X_{MC+Det.Sim.}$ and $X_{MC,had}$ are computed. The correction factor is calculated as

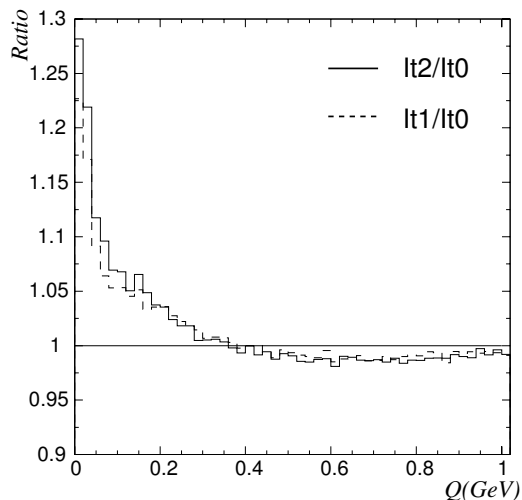$$C := \frac{X_{MC,had}}{X_{MC+det.sim.}} \tag{7.2}$$

Figure 7.1: Increase in pairs with small Q value due to the iterative correction procedure

Application of these factors results in measurements corrected to a well defined particle composition, center of mass energy and with no initial state radiation.

The correction factor C also depends on the MC generator used. A cross-check between different MC programs is therefore desirable. A full detector simulation, however, is a big computational effort. An approximation has to be made, since it is important to at least estimate the model dependency of a certain C.

Instead of using a full detector simulation, only cuts which are used for real events are applied on the MC samples. With this simplified approach a variety of generators can be used to calculate C and the spread in the values of C is taken into account for estimating systematic uncertainties. Comparison to values obtained with full detector simulation shows that the biggest contributions to the overall correction come from cuts on geometry and energy, which are also used for real data (see chapter 5).

7.2   Corrected Q-Distribution

The corrected Q-distribution defined in equation (4.8) is obtained by the procedure described above. For this special case, however, it was found that for small Q values (Q $\approx$ 0.1 GeV) the correction factor is especially dependent on the MC generator and on the choice of parameter values used to create the sample[23]. A so called iterative procedure has to be carried out, beginning with a MC sample (10^6 events) with no BE implementation to correct data. With this lowest order corrected Q-distribution a parameter tuning including BE parameters, as described below, is carried out. The obtained values λ_{BE} and R_{BE} are used to generate a new MC sample ($5 \cdot 10^5$ events) with BE implemented, with which the first (uncorrected) Q-distribution is corrected. This is called *first iteration* of the correction procedure. All steps are repeated again, and a Q distribution, corrected to second order, is obtained. This can be done even further and figure (7.1) shows that the increase in pairs with small Q values ($\approx 0.1 GeV$) from lowest (noBE) to 1st iteration is about 6%. The increase by using 2nd iteration compared to 1st is rather small which makes no further iterations necessary.

This means that if a 0.th order correction procedure is used, the BE effect will be seriously

underestimated. Table (7.1) shows the increase in the BE strength parameter λ_{BE} with higher iterations. Throughout this study, data corrected to second order was used.

iteration	λ_{BE} in MC used for correction	results of tuning for λ_{BE}
0	no BE	0.69
1	0.69	0.99
2	1.00	1.11
3	1.12	1.14

Table 7.1: λ_{BE} for different orders[23]

7.3   Tuning of Parameters of PYBOEI

To get an optimal agreement between data and MC samples, parameters of the simulation have to be tuned. A description of the general tuning procedure in ALEPH can be found in [16]. For the actual fit of parameters, the fortran program LINFIT, as developed inside ALEPH, was used.

The whole procedure will be explained in this section in detail and results will be presented.

7.3.1   Ingredients

In this study 6 parameters were tuned simultaneously. Only two of them are purely BE related. The other 4 are important parameters controlling the hadronization process in the simulation. They are also subject of the tuning because the use of PYBOEI changes event properties. The shift of particles towards each other, for example, leads to jets which are narrower than without BE. To compensate this effect, the parameter σ (see table 7.2) needs to be increased. As a consequence the multiplicity goes down, which makes a rise of A necessary to bring it back up to where it was. Effects like that make a re-tuning of the QCD model parameters of hadronization necessary.

Table (7.2) gives an overview of parameters subject to tuning. The given values correspond to starting points.

PARJ(92)	1.	λ_{BE}, strength of BE effects
PARJ(93)	0.34 GeV	size of the BE effects region in terms of Q
		R$\approx \frac{0.2 GeV fm}{PARJ(93)}$
PARJ(81)	0.30 GeV	Λ_{QCD}
PARJ(82)	1.5 GeV	invariant mass cut-off m_{min} of parton showers,
		below which partons are not assumed to radiate
PARJ(21)	0.38 GeV	σ, width of the gaussian p_x and p_y transverse
		momentum distributions for primary hadrons
PARJ(41)	0.40	parameter a of the symmetric Lund
		fragmentation function

Table 7.2: BE and QCD parameters for tuning

The next ingredient for tuning is a set of measured and corrected distributions derived from $\sim 10^6$ hadronic events of 1994[16] data taking, to which the MC generated ones have to be fitted. In addition to the Q distribution of like and unlike-sign pairs for BE parameters, the following event shape and inclusive distributions were used

- event shape distributions:
  - sphericity S
  - aplanarity A
  - 1-thrust 1-T
  - 3 jet resolution parameter y_3
- inclusive distributions of
  - scaled momentum of charged particles z_{ch}
  - $p_\perp^{in}$ and $p_\perp^{out}$ of charged particles

Figures of all distributions are shown in the result section. Sphericity and aplanarity are obtained from the eigenvalues of the momentum tensor defined as $M_{\alpha\beta} = \sum_i p_{\alpha i} p_{\beta i}$. α and β each refer to the x, y and z components and the sum goes over all selected particles of the event. If Q_j label the normalized eigenvalues of M with $\sum_j Q_j = 1$ and $0 < Q_1 < Q_2 < Q_3$, sphericity and aplanarity are defined as

$$S = \frac{3}{2}(Q_1 + Q_2)$$
$$A = \frac{3}{2}Q_1 \tag{7.3}$$

The corresponding eigenvector $\vec{n}_3$ determines the sphericity axis, $\vec{n}_2$ and $\vec{n}_3$ the event plane. The thrust T is given by

$$T = max \left(\sum_j |p_{\parallel j}| / \sum_j |p_j| \right) \tag{7.4}$$
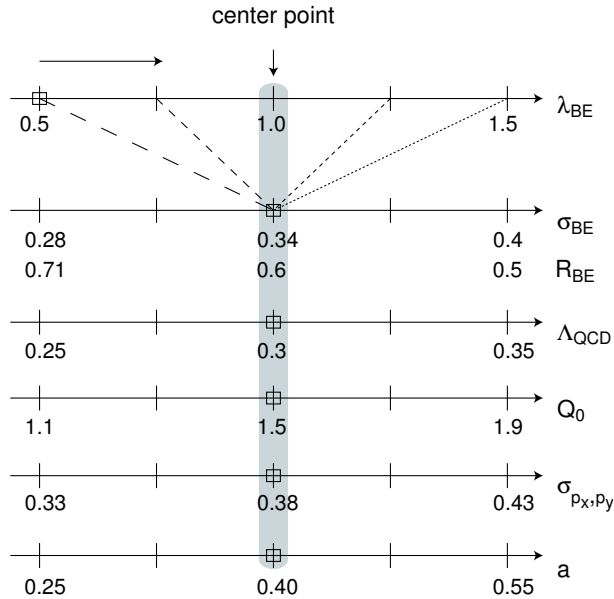
Figure 7.2: Variation of parameters (all in GeV except λ_{BE} and a)

where $p_{\parallel}$ is the momentum along the thrust axis. The event shape variable y_3 is a measure of closeness for 3 jet events. To obtain it a cluster algorithm (DURHAM[24, 25] for this study) has to be used. The algorithm stops when exactly 3 clusters ($\equiv$ jets) remain. The smallest value of y between two of the three jets is the event shape variable y_3.

The inclusive distribution z_{ch} is defined as $\frac{2|\vec{p}|}{E_{cm}}$. Finally $p_{\perp}^{in}$ and $p_{\perp}^{out}$ are the components of a particle's momentum in the event plane and perpendicular to it:

$$p_{\perp}^{in} = |\vec{p} \cdot \vec{n}_2|$$
$$p_{\perp}^{out} = |\vec{p} \cdot \vec{n}_1| \tag{7.5}$$

7.3.2 Tuning Procedure

For the tuning of parameters it is important to know the dependence of a measured quantity M_j (i.e. bin content of bin j) on these parameters. The dependencies, however, are not known in analytical form. It is therefore necessary to calculate these quantities for various values of the chosen parameters to be able to determine a parameterization of the dependency for each bin separately. For practical use it is enough to choose a linear parameterization. The variation of parameters is shown in figure (7.2) and is done as follows. For each parameter x_i a starting value or center point x_{i0} has to be chosen. For our case the starting points for the four non BE related parameters were taken from previous experience, λ_{BE} was set to 1 (chaotic source) and R≈ 0.6 fm. With these 6 initial values a set of 4 million events is calculated and all the histograms are filled. Then each parameter is varied to four other points separately and every time 1 million events are calculated and the histograms are filled. Usually the four additional points are spread around the center point symmetrically at distances of $-\Delta x_i$, $-\Delta x_i/2$, $\Delta x_i/2$ and Δx_i. It is also possible to chose other than those four points if e.g. physical constraints don't allow values on both sides of the central point. The variation range for all six parameters is shown in figure (7.2). For each parameter 4 sets of histograms have to be computed with the

other 5 parameters at their center point. This makes a total of 28 million events for one tuning and means a time of computation on an ATHLON 1800XP between 1 and 3 days depending on the energy conservation method used (BE_{32}, BE_m or BE_λ).

Now the bin content in dependence of the six parameters is known and a linear expression can be fitted for each M_j separately

$$M_j(x_i) = m_j^i + a_j^i(x_i - x_{i0}) \tag{7.6}$$

The best values for the model parameters is found by minimizing the function

$$\chi^2 = \sum_j \left(\frac{M_j^{data} - M_j^{MC}(\vec{x})}{\sigma_j^{data}} \right)^2 \tag{7.7}$$

where the sum goes over all measured quantities, i.e. over all bins and histograms. σ_j^{data} is the quadratic sum of the statistical and systematical error of the data and is much bigger than the MC error, therefore the latter can be neglected. The statistical error of $\frac{1}{N}\frac{dn}{dQ}$ was multiplied by an arbitrary factor 2 because no systematic errors were available.

If the tuned parameters exceed a linear range which is calculated according to the goodness of the parameterization (7.6), the tuning has to be repeated by shifting the central points x_{i0} according to the last results. This type of fit (7.7) assumes that the experimental data points are uncorrelated, which does not need to be true in general and therefore the errors on the results can only be regarded as a rough measure of uncertainty. The tuning was repeated until all parameters were within the given linear range.

7.3.3 Results for PYBOEI

In this section results of the tuning of the six parameters of table (7.1) are presented. Three different methods, namely BE_{32}, BE_m and BE_λ (see chapter 6), with two different basic parameterizations (gaussian and exponential) each, were used and parameters were adjusted.

Figures (7.3) and (7.4) show the 4 event shape distributions S, A, $1-T$ and y_3 and the 3 inclusive hadron spectra z_{ch}, $p_{t,in}$ and $p_{t,out}$ for all three energy conservation methods BE_{32}, BE_m and BE_λ for a gaussian parameterization. Figures (7.5) and (7.6) show the according graphs for an exponential parameterization.

For $p_{t,out}$ and aplanarity A (and also for the Q distributions) not all bins were used for the tuning. A line with an arrow indicates the bins which were included.

There is a good agreement between data and MC if you only look at bins used for the tuning. For higher values of A and $p_{t,out}$ (and also for z_{ch}), BE_m and BE_λ show better agreement with data than BE_{32} does. When it comes to the simulation of the BE effect, however, we will see that BE_{32} gives the best results.

Final BE results for all methods are shown on the subsequent pages.
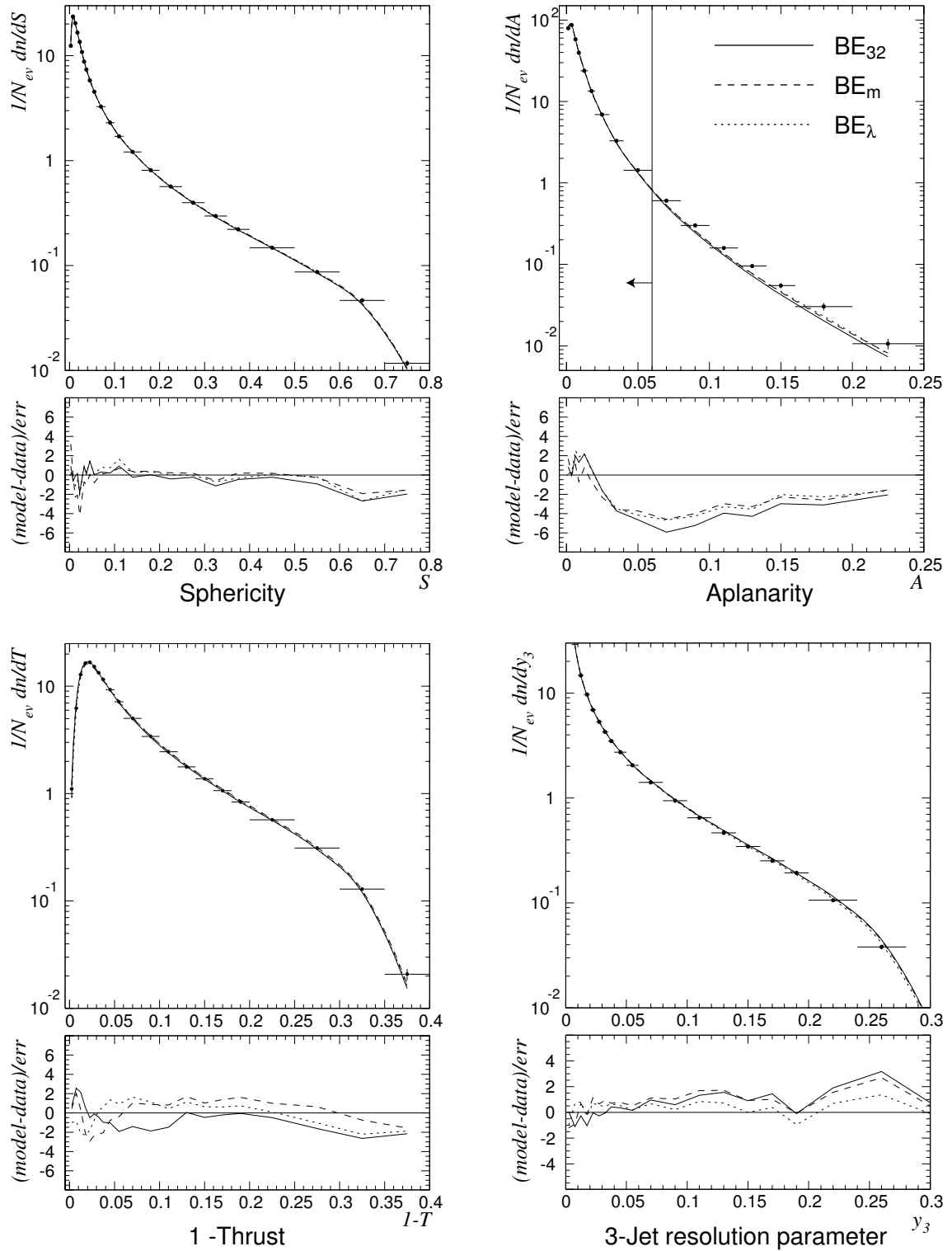
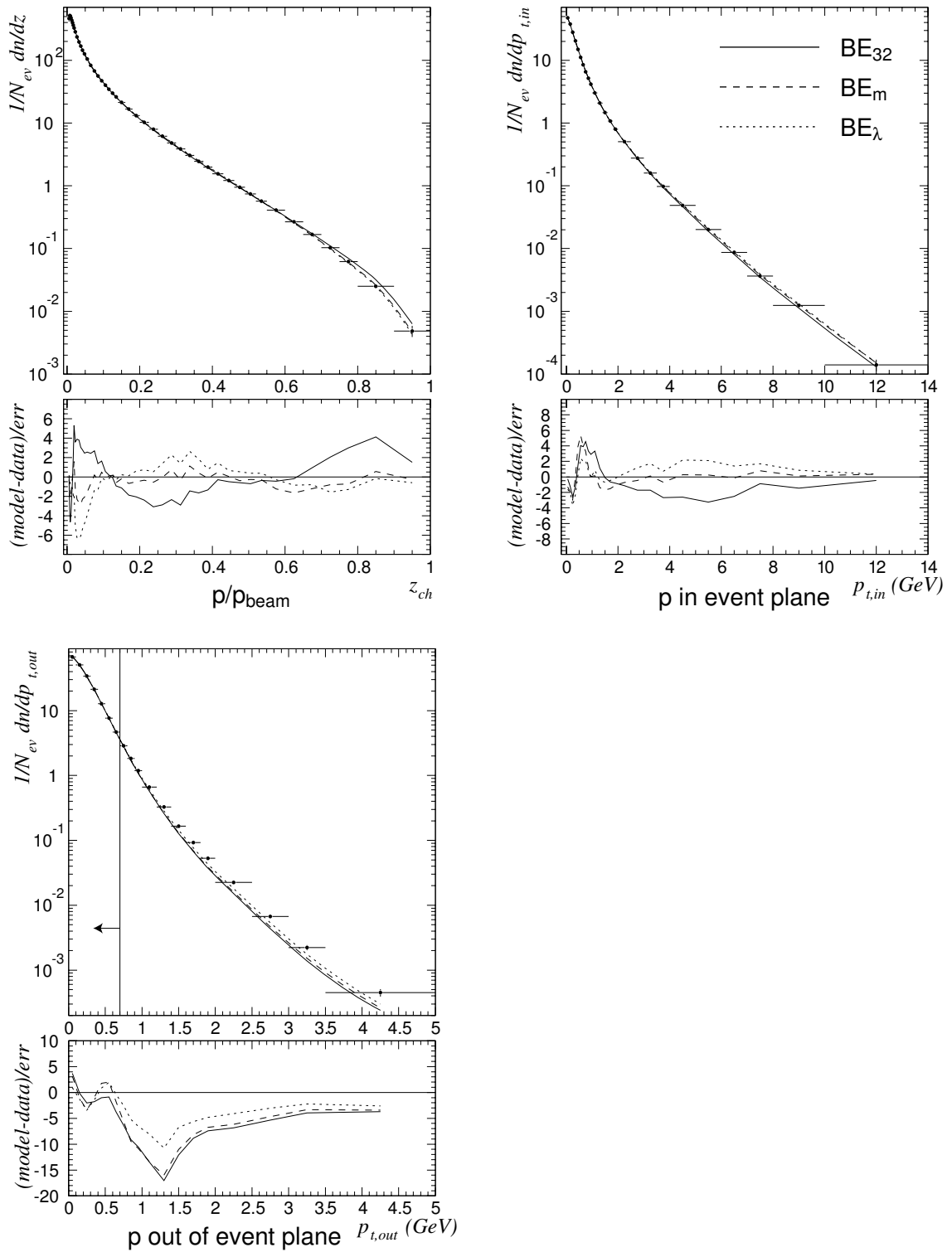Figure 7.3: Event shape distributions for gaussian parameterization

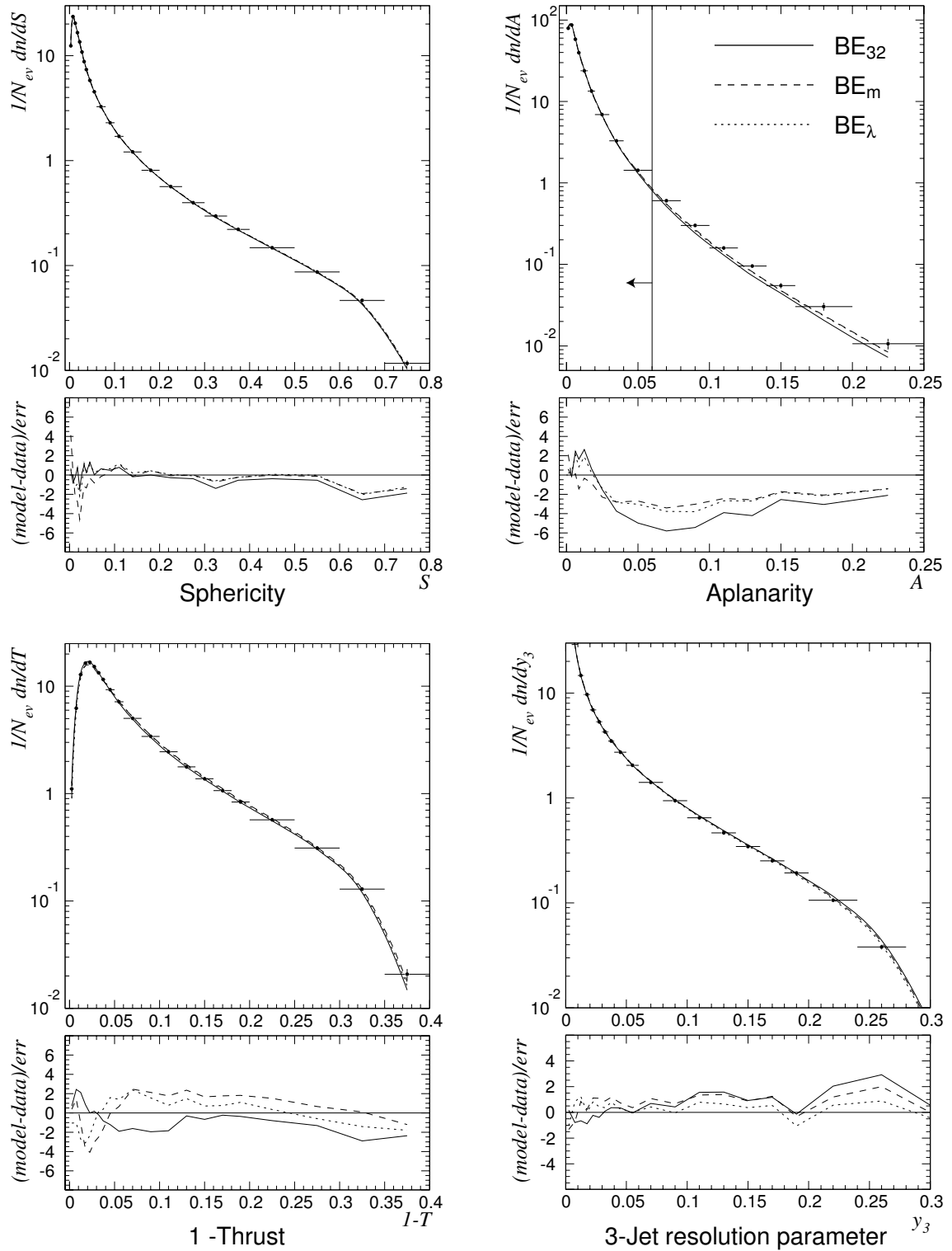Figure 7.4: Inclusive distributions for gaussian parameterization

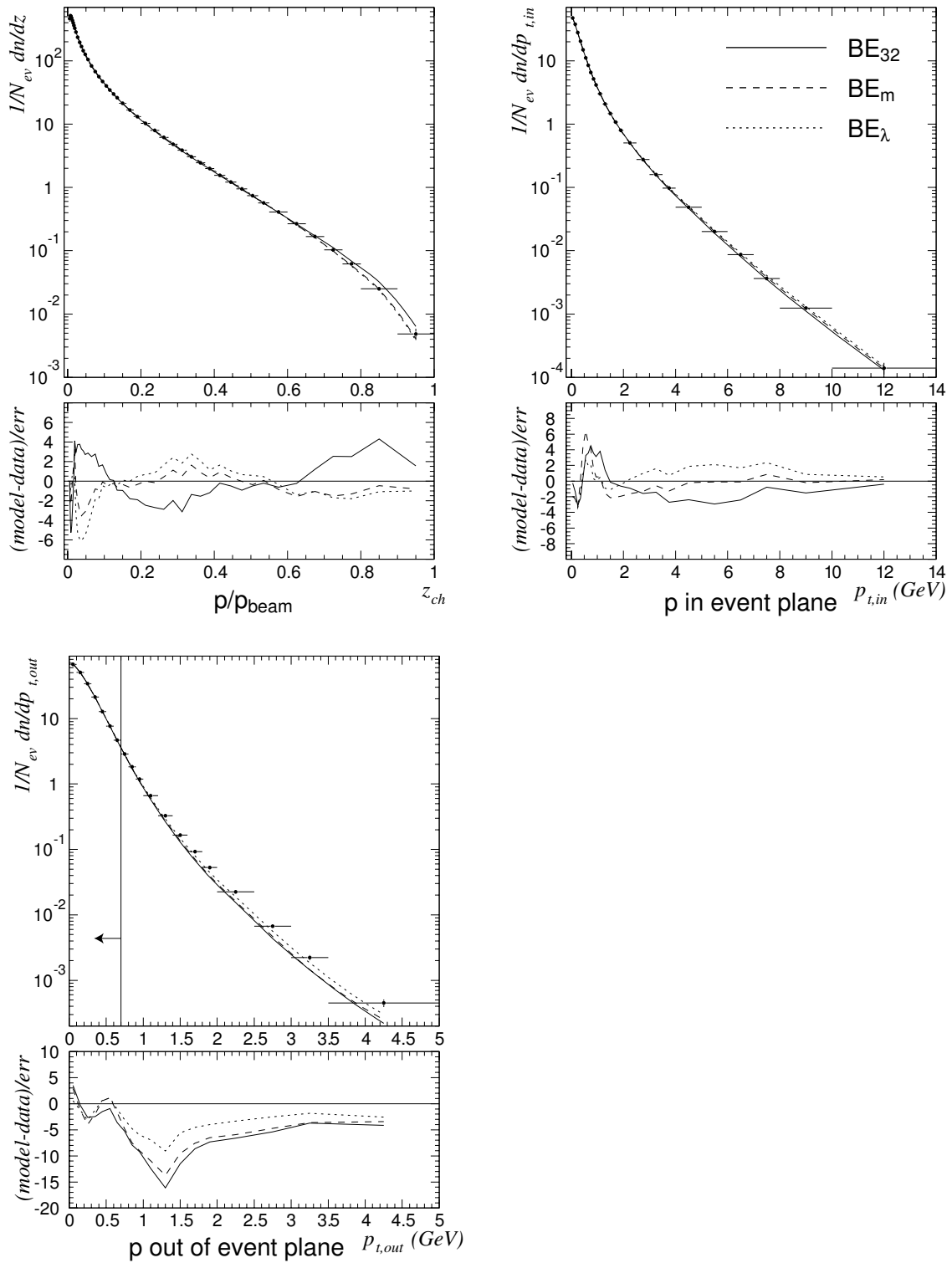Figure 7.5: Event shape distributions for exponential parameterization

Figure 7.6: Inclusive distributions for exponential parameterization

Results for BE$_{32}$

Figure (7.7) shows the final correlation function, as defined in (4.9), for the BE$_{32}$ algorithm in comparison with corrected data (crosses). The region used for tuning is indicated by a line with arrows. The table below provides information about the numerical values of the tuned parameters. In addition, values for the four non BE related parameters Λ_{QCD}, Q_0, σ and a which come from a tuning with no BE effect implemented, are given.
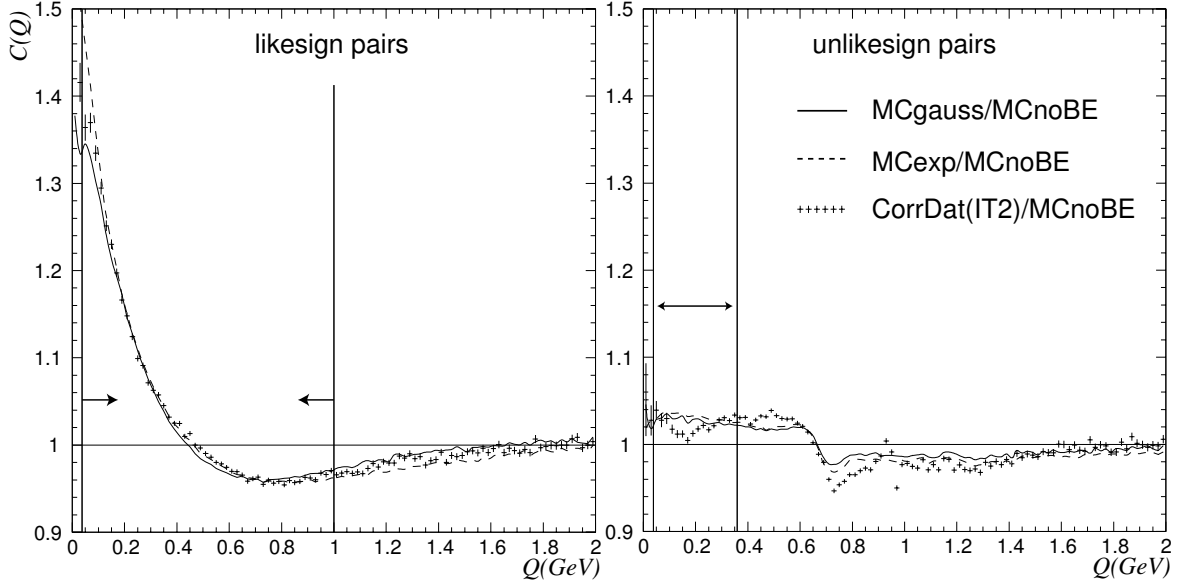
Figure 7.7: BE$_{32}$ like-sign and unlike-sign Q-distributions

	λ_{BE}	R_{BE} $[fm]$	Λ_{QCD} $[GeV]$
gauss	1.135 ± 0.030	0.606 ± 0.011	0.291 ± 0.002
exp	1.799 ± 0.067	0.788 ± 0.020	0.292 ± 0.002
noBE			0.285
	Q_0 $[GeV]$	σ $[GeV]$	a
gauss	1.493 ± 0.051	0.377 ± 0.002	0.429 ± 0.014
exp	1.513 ± 0.053	0.385 ± 0.002	0.446 ± 0.014
noBE	1.32	0.366	0.365

Table 7.3: Results for BE$_{32}$

Results for BE$_m$

Results for BE$_m$ are shown in figure (7.8), below are the values of the tuned parameters.
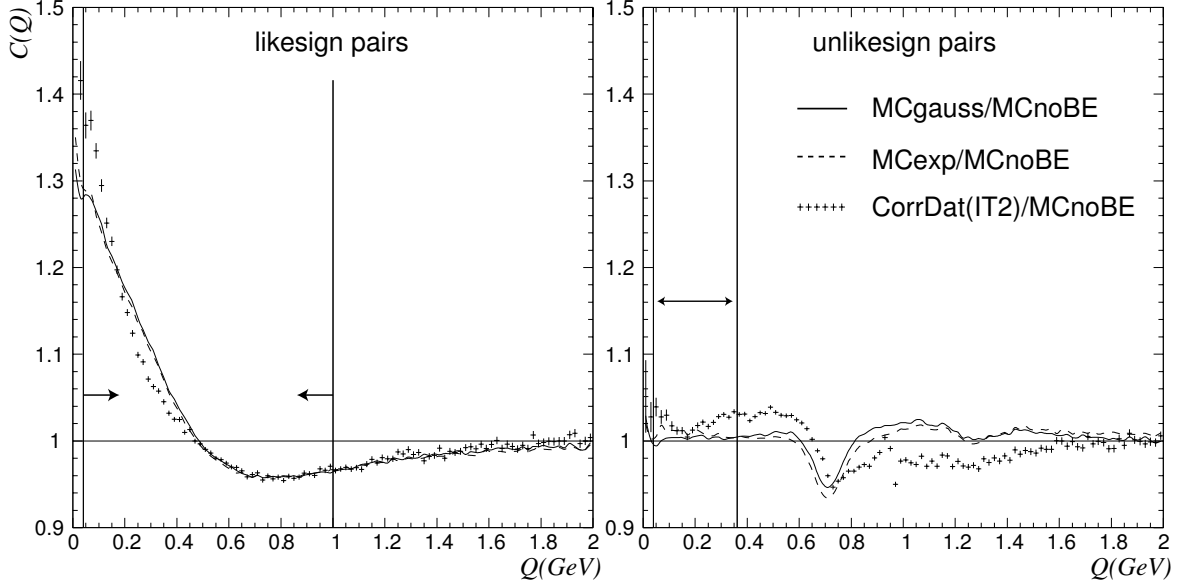
Figure 7.8: BE$_m$ like-sign and unlike-sign Q-distributions

	λ_{BE}	R_{BE} $[fm]$	Λ_{QCD} $[GeV]$
gauss	0.691 ± 0.010	0.347 ± 0.005	0.289 ± 0.002
exp	0.748 ± 0.010	0.366 ± 0.005	0.280 ± 0.002
noBE			0.285
	Q_0 $[GeV]$	σ $[GeV]$	a
gauss	0.771 ± 0.026	0.304 ± 0.002	0.103 ± 0.010
exp	0.677 ± 0.027	0.282 ± 0.002	0.051 ± 0.009
noBE	1.32	0.366	0.365

Table 7.4: Results for BE$_m$

Results for BE$_\lambda$

Figure (7.9) shows the results for BE$_\lambda$. Table (7.5) contains the numerical values of the tuned parameters.
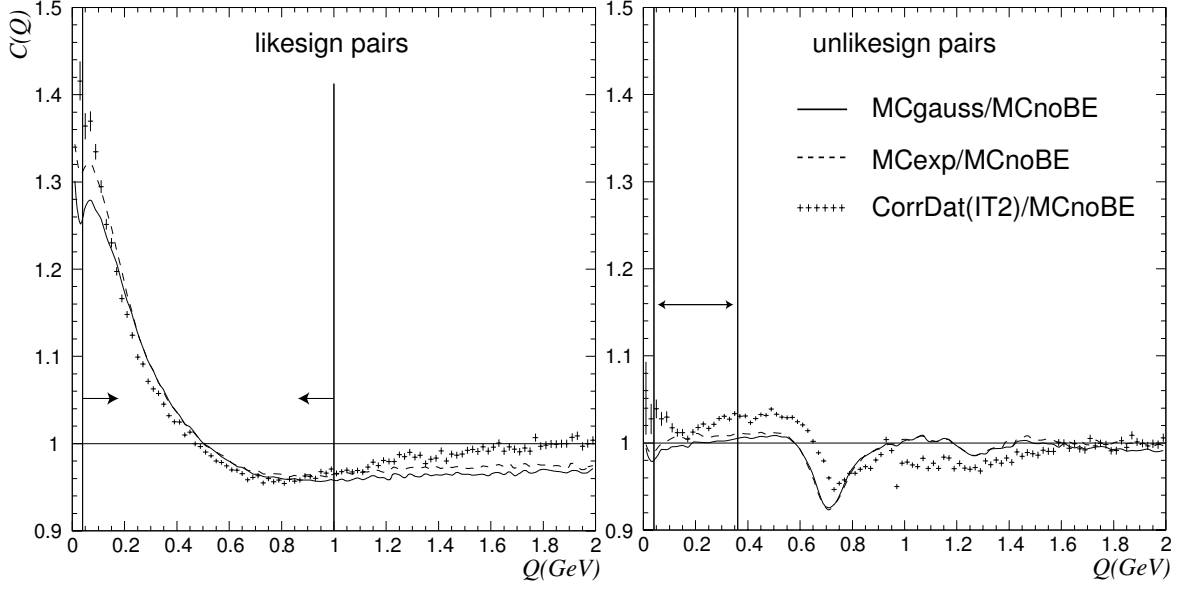
Figure 7.9: BE$_\lambda$ like-sign and unlike-sign Q-distributions

	λ_{BE}	R_{BE} [fm]	Λ_{QCD} [GeV]
gauss	0.479 ± 0.008	0.193 ± 0.003	0.290 ± 0.002
exp	0.571 ± 0.008	0.195 ± 0.003	0.286 ± 0.002
noBE			0.285
	Q_0 [GeV]	σ [GeV]	a
gauss	0.739 ± 0.030	0.352 ± 0.002	0.187 ± 0.011
exp	0.680 ± 0.028	0.342 ± 0.002	0.162 ± 0.014
noBE	1.32	0.366	0.365

Table 7.5: Results for BE$_\lambda$

7.3.4 Discussion of Results

The preceding three pages show that BE_{32} gives the best description of the like and unlike-sign Q-distributions. BE_m and BE_λ, however, are not useful when BECs are to be simulated. The goodness of the fits (table 7.6) underlines this. χ^2 values for the Q-distributions of BE_m and BE_λ are higher by a factor of 4 to 6 compared to BE_{32}. Due to the somewhat better description of the event shapes and inclusive distributions by BE_m and BE_λ compared to BE_{32}, the overall goodness (= sum over all χ^2) of the latter is only a bit better than that of the first two.

	Q like-sign	Q unlike-sign	$\sum \chi^2$	$\left(\sum \chi^2\right)/n_{dof}$
BE_{32} gauss	61.5	36.9	675.3	3.08
BE_{32} exp	34.6	41.5	672.7	3.07
BE_m gauss	353.2	164.6	875.3	3.99
BE_m exp	296.5	113.1	901	4.11
BE_λ gauss	247.3	144.7	850.2	3.88
BE_λ exp	135.1	123.5	705.8	3.22
# bins	48	16	225	

Table 7.6: Value of χ^2 for the different methods

The best agreement is achieved with BE_{32} and an exponential parameterization which is a bit better than the gaussian one. BE_m with a gaussian parameterization yields the worst agreement.

When a gaussian parameterization is used, a theoretical range for $\lambda_{BE} \in [0, 1]$ was given in section (4.1). The tuned value of λ_{BE} for BE_{32} lies a bit above unity ($\lambda_{BE} \approx 1.1$). This cannot be viewed as a violation of the allowed range, because λ_{BE} is, primarily, a model parameter tuned to describe data best. To reach this goal, it turns out that it has a value above 1.

The QCD related parameters Λ_{QCD} and σ only differ a bit from noBE values. Λ_{QCD} turns out to be quite stable for all BE methods and σ has its highest deviation from noBE value for BE_m with exponential parameterization (about 20% lower). Q_0 and a are comparable in size with noBE values for the BE_{32} algorithm, which is a good sign for its applicability to implement BECs into MC samples. For BE_m and BE_λ these two parameters differ a lot from the noBE case (e.g. a of BE_m with exponential parameterization is only about 14% of the noBE value!).

The residual BE effect (see section 4.3) in unlike-sign pairs is reproduced, at least qualitatively, by all three algorithms. Here, best agreement is achieved (see χ^2 of Q unlike-sign in table 7.6) with BE_{32} and a gaussian parameterization.

The correlation coefficients for BE_{32} between λ_{BE}, σ_{BE} and the four QCD parameters is given in table (7.7). R_{BE} and σ_{BE} are related via $R_{BE} = \hbar/\sigma_{BE} \approx (0.2 \text{ fm GeV})/\sigma_{BE}$.

	λ_{BE}	σ_{BE}	Λ_{QCD}	Q_0	σ	a
gaussian						
λ_{BE}	1.	-0.769	-0.036	0.018	-0.062	0.016
σ_{BE}	-0.769	1.	-0.049	0.110	0.441	0.228
exponential						
λ_{BE}	1.	-0.867	-0.051	0.005	-0.120	-0.009
σ_{BE}	-0.867	1.	-0.006	0.080	0.415	0.183

Table 7.7: Correlation coefficients for tuned parameters of BE_{32}

A strong negative correlation exists between the two BE parameters λ_{BE} and σ_{BE}. The biggest correlation between a BE and QCD related parameter is that between σ_{BE} and σ (≈ 0.4). Among other parameters no correlation larger than 0.3 exists.

Reasons for a better performance of one algorithm compared to another are not all clear. The 3 methods are based on the same principle of shifting particle momenta apart of or towards each other. The only difference lies in energy conservation. Nevertheless all 3 are a purely phenomenological post-processing of what really happens when the identical bosons are produced. It also cannot be said in general that one is more appealing theoretically than the other. The more troublesome approaches of purely local energy conservations (see chapter 6) among 4 *close* particles of BE_m and BE_λ may give hint that these methods might be worse.

7.4 "Tuning" of Parameters of K+K

7.4.1 Adjustment of $\langle \omega \rangle$

The adjustment of MC to data for the K+K model is somewhat different compared to PY-BOEI/PYTHIA. An advantage over other global event weighting models is that the weight w for a single event can also be below 1. This makes it possible that the average event weight can be adjusted to unity. If $\langle \omega \rangle$ is about unity it is hoped that average event quantities (like average multiplicity) or distributions on parton level (e.g. initial quark flavor distribution) are left unchanged. As we will see in the result section, this is unfortunately not the case.
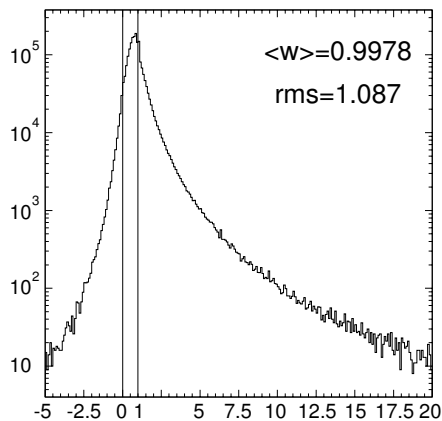

Figure 7.10: Event weight distribution for R=0.667 fm, $d_{max} = 40$ fm

To adjust $\langle \omega \rangle$, for a given set of BE parameters R, d_{max} and n_{max}, one single parameter ξ is used[21]. This value determines where the parameterization (6.19) goes below unity. To find a good value for ξ is a time consuming task and is done by trial and error. For an arbitrary value of ξ, let the simulation run, look at the event weight distribution and at the average weight and then change ξ accordingly and do it all over. The dependence of $\langle \omega \rangle$ on ξ is not linear. This makes it harder to guess how to change ξ so that after the next run $\langle \omega \rangle$ is closer to unity than before.

Figure (7.10) shows an event weight distribution for R=0.667 fm, $d_{max} = 40$ fm and by use of cluster method 1. The average weight is $\langle \omega \rangle = 0.9978$ with a *rms* of 1.087. Events with a large weight have a bigger influence on the average event weight than those closer to unity. Therefore a cut is used which excludes events with a weight bigger than 20. This affects only 0.05% of all events and it is reasonable not to take those into consideration since they only seem to have a (coincidentally) special combination of kinematics and number of identical bosons which makes the weight that high. These events show otherwise no special behavior and would unnecessarily shift the average event weight of the distribution so that another, for most events *wrong* ξ would be used.

7.4.2 Results for K+K

The adjustment of $\langle \omega \rangle$ to unity has been done for several values of R and d_{max} (see table 7.8). A value of 0.9 fm for R is the default used by K+K, 0.667 fm comes from PYBOEI results which are around 0.6 to 0.8 (for BE_{32}). Keep in mind that the R of K+K is not identical to the R_{BE} of PYBOEI due to the a priori different algorithms. Therefore R values obtained from PYBOEI cannot be directly compared to those used here but can only be taken as a suggestion.

method	1					
$d_{max}[fm]$	10		40		80	
R[fm]	0.667	0.9	0.667	0.9	0.667	0.9
ξ	1.12	0.99	1.18	1.04	1.20	1.06
$\langle \omega \rangle$	0.99	1.00	1.00	1.00	1.00	1.00

method	2					
$d_{max}[fm]$	10		40		80	
R[fm]	0.667	0.9	0.667	0.9	0.667	0.9
ξ	1.02	0.92	1.07	0.96	1.08	0.97
$\langle \omega \rangle$	1.00	1.00	1.00	1.00	1.00	1.00

Table 7.8: Parameter settings with corresponding ξ and $\langle \omega \rangle$ values

On the following pages results for the K+K algorithm are presented.
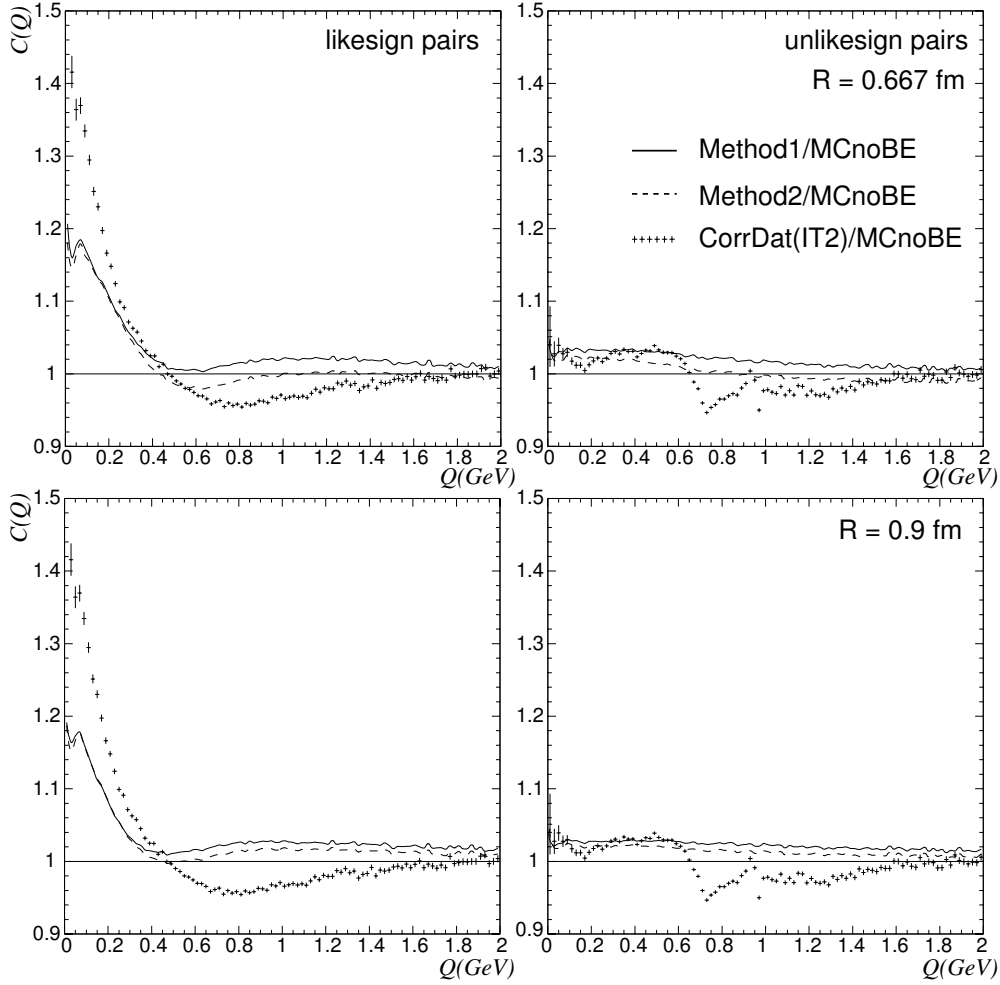
Results for $d_{max} = 10$ fm

Figure 7.11: Q-distributions for $d_{max} = 10$ fm

The like-sign distributions for both R=0.667 fm and R=0.9 fm show a clear rise towards smaller Q values. Due to the small $d_{max} = 10$ fm only 42% of all identical bosons participate in BE. Hence, the BE effect is not reproduced to full scale. Agreement with data is, for all values of Q, rather bad.

The unlike-sign Q-distribution shows good agreement up to Q $\approx$ 0.6 GeV. The change of Q values of resonance decays due to the residual BE effect (see section 4.3) shown by the data (bump at around 0.7 GeV) is not reproduced at all.
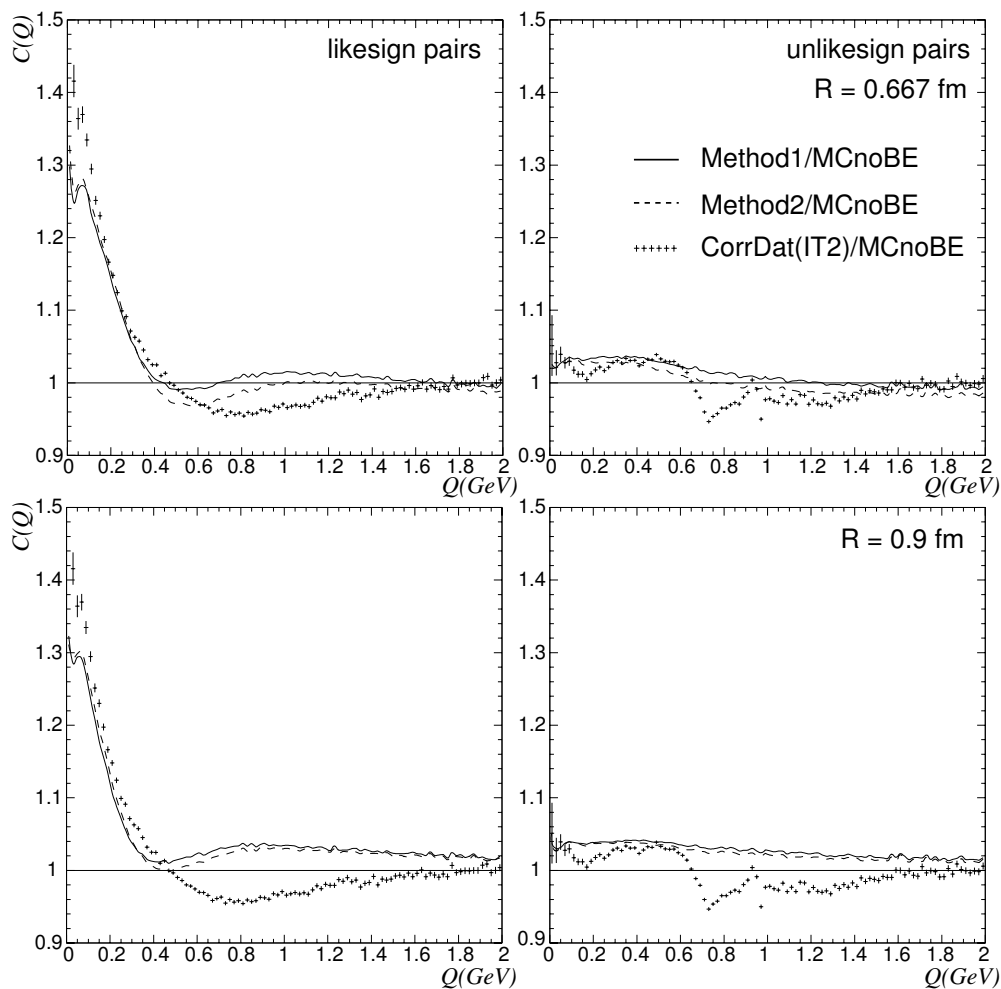
Results for $d_{max} = 40$ **fm**

Figure 7.12: Q-distributions for $d_{max} = 40$ fm

With a higher value of $d_{max} = 40$ fm more bosons (58%) participate in BE and the rise towards smaller Q values gets bigger. A bad behavior for intermediate Q values remains.

The disability of describing the shift in Q values of resonance decays remains and seems to be parameter independent. It can be viewed as a general shortcoming of this algorithm.
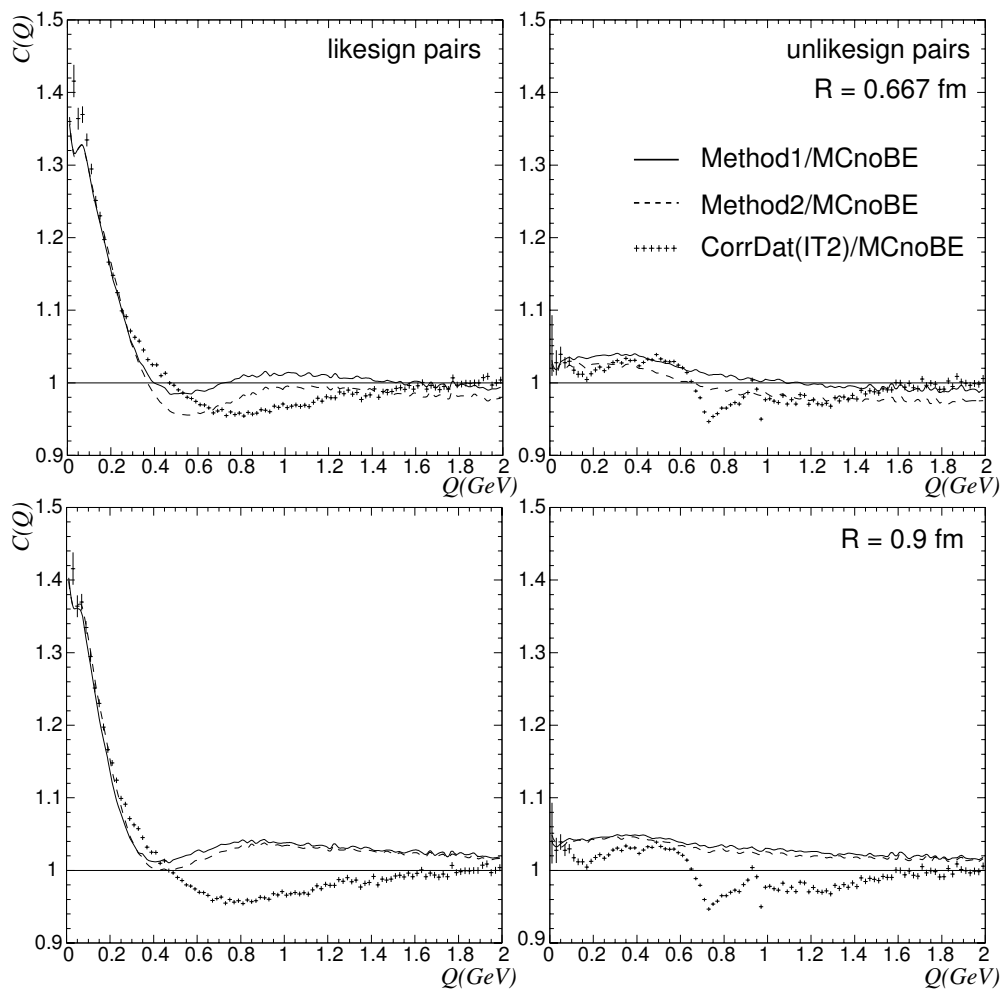
Results for $d_{max} = 80$ fm

Figure 7.13: Q-distributions for $d_{max} = 80$ fm

With $d_{max} = 80$ fm, the BE effect is reproduced almost to its full strength. Best agreement is achieved with R=0.667 fm and cluster method 2, which also better describes the dip below unity for intermediate values of Q.

Again, the shift in Q values of resonance decays is not reproduced.

7.4.3 Discussion of Results

The obtained results show that this method might be capable of describing BECs in multi-hadronic Z decays. The adjustment of the average event weight $\langle \omega \rangle$ to unity for every set of parameters is a troublesome attribute of this algorithm and has to be done *by hand*. In that sense a tuning as carried out for PYBOEI is not really possible. Only a few sets of parameter values were used and the resulting Q-distributions compared to data. Therefore, it is very well possible and likely that with other values a better agreement with data can be achieved. Some shortcomings of the algorithm, however, seem to be independent of this choice.

Best agreement is achieved for $d_{max} = 80$ fm. The choice of R doesn't have much impact on the results for small Q values, and the type of cluster method used neither. For intermediate values of Q, cluster method 2 with R=0.667 fm shows a better behavior when it comes to describe the slight dip below unity. Nevertheless, if compared to BE$_{32}$ of PYBOEI, the result can only viewed as being satisfactory for values of Q smaller than 0.3 GeV.

Despite of this small success, this method also causes some problems when it comes to the description of resonance decays or fundamental things like the factorization property of QCD.

First, the Q value of decay products of resonances like $\rho \rightarrow \pi^+\pi^-$ is almost a constant quantity given by (6.1). *Almost*, because $\Gamma_\rho \sim 150$ MeV[1]. After the production of the $\pi^+\pi^-$ pair, BE effects can change the Q value if another identical boson, in this case a π^+ or a π^-, is close by in momentum space ($\rightarrow$ residual BE effect). The results show that the model of K+K ignores this influence of the BE effect on the unlike-sign distribution. The bump at Q around 0.7 GeV as seen for data is not reproduced by the simulation, independent of the set of parameters used. Second, if the global event weight is applied on parton level distributions like
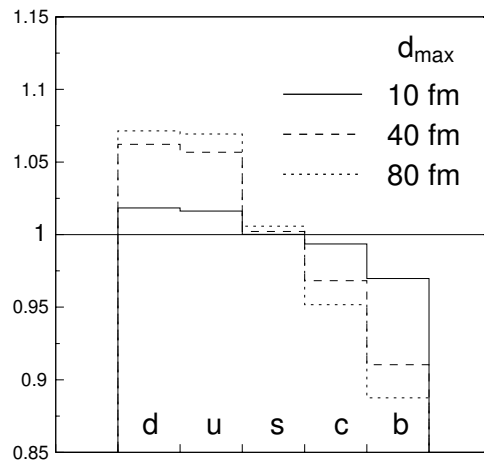

Figure 7.14: Changed flavor composition due to global event weight

the initial quark flavor distribution, the cross sections of the decay of the Z into the five possible types of quarks (d, u, s, c and b) is changed, despite the fact that $\langle \omega \rangle$ was adjusted to unity. The same is unfortunately true for other average event quantities (see below). Figure (7.14) shows the initial quark flavor composition after the global event weight has been applied divided by an un-weighted noBE sample. The parameter setting which leads to the best agreement with data unfortunately shows the biggest change in the initial quark flavor composition. After the weighting, events with $b\bar{b}$ as the primary quark pair are reduced by about 12% ($c\bar{c}$ events by about 5%). This is a violation of the concept of factorization which should hold during the

whole process of hadronization. In principle a smaller weight for $b\bar{b}$ (or $c\bar{c}$) events would be alright because it is known that the BE effect in those events is less than for events with d, u or s as the primary quark pair. Because of the relatively long lifetime of B and C mesons ($\rightarrow$ weak decays, $\tau \approx 10^{-12}$ sec) their decay products do not participate in BE anymore and the overall BE effect is reduced.

Other average event quantities like average multiplicity are also changed by this global event weighting procedure. Table (7.9) shows some average values for the case of $d_{max} = 80$ fm and $R = 0.667$ fm.

	no weight	K+K	change in %
$\langle N_{ch} \rangle$	18.2	18.49	+ 1.6%
$\langle S \rangle$	0.07591	0.07069	- 6.9%
$\langle A \rangle$	0.01176	0.01133	- 3.7%

Table 7.9: Average event values before and after the global event weight is applied

7.5 PYBOEI vs. K+K

In summary, the only method which is in satisfactory agreement with data over a wide range of Q values is the BE_{32} algorithm of PYBOEI. Neither BE_m/BE_λ nor K+K (no matter which parameter setting tried) show a comparable good result.

A general advantage of PYBOEI over K+K is that a tuning of parameters is very well possible, which helps a lot to achieve good or even the best results possible for a given algorithm. This doubtlessly outbids the disadvantage of a necessary re-tuning of QCD parameters, because BE parameters have to be tuned anyway. By doing so, QCD parameters can be determined as well.

Another benefit of PYBOEI is that it is also capable of describing the change in Q values of resonance decays due to the residual BE effect, which is measured in unlike-sign Q-distributions. K+K does not show any change concerning the Q values of resonance decays.

A global event weighting routine, like the one from K+K, is an a priori problematic algorithm because one must be aware that the global weight has to be applied on every quantity of an event. This implies that some (especially parton level) distributions will be changed afterwards even with the adjustment of an average weight to unity. But one has to decide if a slight change of parton level distributions (i.e a *slight* violation of factorization) can be accepted, if in return it is possible to get a good agreement with data for the BE effect, without having the problems of total energy conservation PYBOEI has.

As a result it can be said that for further studies which need to include BECs it is advisable to use PYTHIA's built in routine PYBOEI with BE_{32} option and the parameter settings presented.

At last, to defend the K+K algorithm it needs to be said that it is still under development. The version studied in this thesis is not up to date anymore. Since the aim of this diploma thesis is the study and comparison of different BE algorithms I had to agree on one K+K version back then, knowing that it won't be up to date by the time writing the thesis.

Chapter 8

Further Checks of PYBOEI

In the preceding chapter we saw that the BE_{32} option of PYBOEI describes the BE effect observed in the Q-distribution of identical bosons, which come from hadronic Z^0 decays, quite well. For the study of fully hadronic W^+W^- events (i.e. $e^+e^- \to W^+W^- \to hadrons$) at LEP-2 the center of mass energy of the colliding electron-positron pair was raised to $E_{cm} \approx$ 200 GeV. Most of these events are so called 4-jet events. However, not all of the selected events are fully hadronic W^+W^- decays, about 15% come from hadronic Z^0 events with a 4-jet topology (i.e. $e^+e^- \to Z^0 \to hadrons(4jet)$)[27]. This background has to be subtracted for the analysis of fully hadronic W^+W^- decays and therefore it is important to know if the BE effect is also reproduced in 4 jet hadronic Z^0 decays by simulation.

The number of jets an event has is dependent on the jet algorithm and its parameters. For this study the DURHAM[24, 25] algorithm with y_{cut}=0.01 was used.

In this chapter the ratio C(Q) (see 4.9) of 2, 3 and 4 jet events of hadronic Z^0 decays, obtained by MC simulation, was compared to the ones obtained from data. Here $E_{cm} = M_Z$, but it is assumed that the results are also valid for $E_{cm} \approx$ 200 GeV.

For the tuning of the six parameters which was done on hadron level, the data had to be corrected for detector related effects, i.e. brought from detector level to hadron level. Corrected Q distributions for the different 2, 3 and 4 jet events are not available and therefore the MC analysis is moved from hadron level to detector level. Up to now the MC simulation is free of detector related effects. It has to be sent through a detector simulation (see section 7.1). For clarity, figure (8.1) shows the connection between the two different levels.
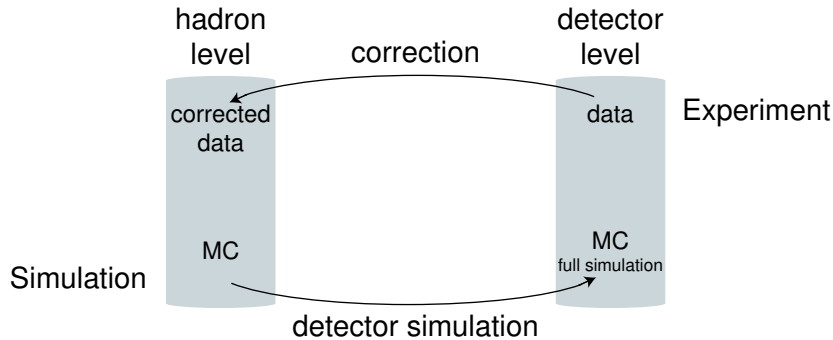

Figure 8.1: Connection between hadron and detector level

A fully simulated MC sample (PYBOEI with BE_{32} and a gaussian parameterization) with $\lambda_{BE} = 1.12$ and $R_{BE} = 0.604$ fm according to iteration 3 in table (7.1) was chosen. The values of λ_{BE} and R_{BE} are very close to the ones found in this study ($\lambda_{BE} = 1.13$, $R_{BE} = 0.606$ fm). The ratio C(Q) of like-sign bosons for all events and for 2, 3 and 4 jet events were compared with data and are presented in figure (8.2).

The ratio C(Q) for all events is also reproduced on detector level. Just like in figure (7.7), the BE effect, when implemented with a gaussian parameterization, is a little bit smaller than that of data. More interesting, BE effects in 2 to 4 jet events, to which the model was not tuned, are also reproduced. BE in 3 jet events is simulated best, in 4 jet events it is a bit overestimated and in 2 jet events it's a bit too small. Since about 70% of all events are 2 jet events, the ratio C(Q) for all events lies a bit below data. Even though for the simulation of BE effects in hadronic Z^0 events the BE_{32} option of PYBOEI shows best agreement of all the different methods tried, this result shows that it is not perfect either. The K+K algorithm was not tried for 2 to 4 jet events separately and therefore no statement about its performance for this case can be made.
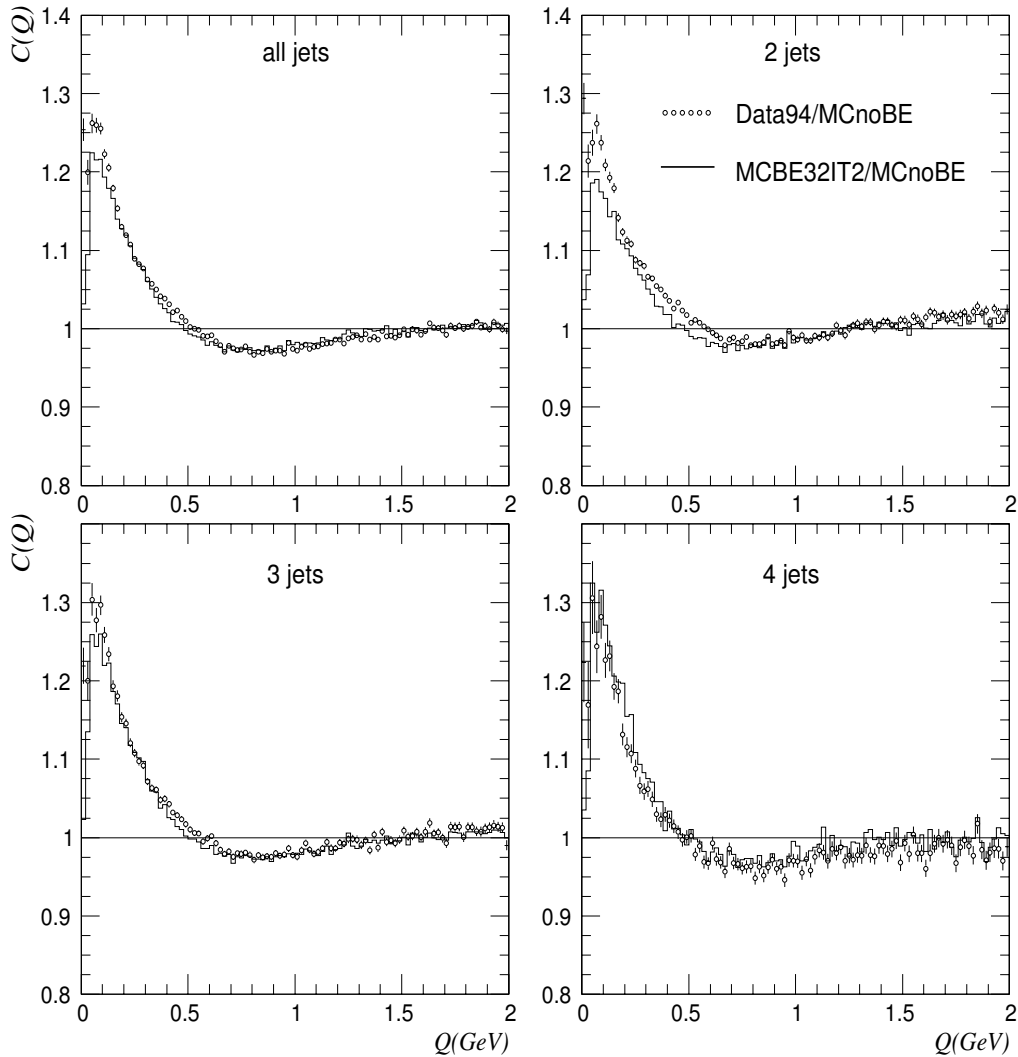

Figure 8.2: BE effect in n-jet topologies

Chapter 9

Summary

The aim of this thesis was the study and tuning of different algorithms which try to implement the Bose-Einstein effect into MC simulations.

Theory of the Bose-Einstein effect predicts an enhancement in the production of pairs of identical bosons which are close in phase space. A sensitive quantity to measure this effect is the so called Q-distribution of identical bosons. Particles which are close in phase space have a small Q value. To make the BE effect *visible* the Q-distribution of identical particles is divided by a Q-distribution of a so called reference sample which is assumed to be free of BE effects. This ratio is called the correlation function C(Q). Different choices of reference samples are possible (see section 4.3). For this study it was obtained by a MC simulation with no BE simulation implemented. A rise in the C(Q) distribution of data towards smaller Q values (see figure 5.1) is taken as evidence for the existence of BE effects. Since the reference sample was only used to visualize the BE effect by calculating the ratio C(Q), its choice has no effect on the parameters fitted in this study.

To implement the BE effect into MC simulations two different methods were used:

- PYBOEI, a momentum shift method together with local conservation of energy. It is part of the event generator PYTHIA[2] (but turned off by default).

- A routine written by V.Kartvelishvili and R.Kvatadze which makes use of the concept of a global event weighting scheme proposed by B. Andersson and M. Ringner[9].

For both, the event generator PYTHIA 6.152 was used (for K+K with PYBOEI turned off) and 9 different quasi-stable bosons were subject to BE: π^+, π^-, π^0, K^+, K^-, K_S^0, K_L^0, η and $\eta\prime$ ($\rightarrow$ about 80% of all charged particles in the final state are pions!).

Corrected data from 1994 with 1 million hadronic Z^0 events ($e^+e^- \rightarrow Z^0 \rightarrow hadrons$) was provided by the ALEPH collaboration.

In PYBOEI, the change in the Q value of identical pairs due to the BE effect has to be translated in a change of the 4-vector p of each particle. The choice is made that momentum is conserved. As a consequence energy is not conserved anymore. PYBOEI offers different options to restore energy conservation. Three of them were tried: BE_{32}, BE_m and BE_λ. For all three a gaussian and an exponential parameterization was considered. A simultaneous

tuning of 6 model parameters was carried out: 2 BE related parameters (R_{BE}, λ_{BE}) and 4 model parameters (Λ_{QCD}, Q_0, σ and a), which are important parameters controlling the hadronization process. In addition to the two Q-distributions (like and unlike-sign), 7 other event and inclusive distributions (see chapter 7) were used to tune the 6 parameters. The tuning of BE_m and BE_λ was done here for the first time in ALEPH.

For the BE routine of K+K, different sets of model parameters R_{BE}, d_{max} and 2 cluster methods (see table 7.8) were tried. The ratio C(Q) of the like-sign Q-distribution was calculated and compared to that of data. A genuine multi-dimensional tuning for the two BE parameters R_{BE} and d_{max} was not possible due to the different scheme of computation.

Best results were obtained with the BE_{32} option of PYBOEI (see figure 7.7). Not only the enhanced production of identical bosons with small Q values (Q $\lesssim$ 0.5 GeV) due to the BE effect is reproduced, there is also good agreement between the MC Q-distribution and that of data for intermediate and larger values of Q up to 2 GeV.

The K+K algorithm did not show good agreement with data for most parameter values tried. For one parameter setting (R=0.667 fm, d_{max}=80 fm), the enhanced production of pairs of identical bosons with small Q values (Q $\lesssim$ 0.3 GeV) due to the BE effect was reproduced. For Q values of the like-sign Q distribution above 0.3 GeV the agreement with data is bad. In addition, for this parameter setting, it was found that distributions at parton level (e.g. the initial quark flavor distribution) were changed. The cross section of $b\bar{b}$, for example, was reduced by 12%. This is a violation of the important concept of factorization of QCD.

The BE effect also changes the Q-distribution of unlike-sign pairs. This is called residual BE effect. A part of this effect is the change of Q values of resonance decays. All energy conservation options of PYBOEI (BE_{32}, BE_m and BE_λ) reproduce the residual BE effect observed in the unlike-sign Q-distribution. The algorithm of K+K is not capable of doing so. It is in rather good agreement for Q values smaller than 0.6 GeV but in bad agreement for values above. A shift in the Q values of resonance decays is not described at all.

The overall result is, that it is advisable to use the PYTHIA built-in routine PYBOEI with option BE_{32} and parameters presented whenever it is necessary for the analysis to take BE effects into account.

Bibliography

[1] Particle Physics Booklet, extracted from K. Hagiwara *et al.*, Physical Review **D66**, 010001 (2002)

[2] T. Sjöstrand, P. Eden, C. Friberg, L. Lönnblad, G. Miu, S. Mrenna and E. Norrbin, PYTHIA 6.2 Manual, Computer Physics Commun. **135** (2001) 238.

[3] B. Greene, The Elegant Universe, Vintage Books, USA 2000

[4] E. Lohrmann, Hochenergiephysik, Teubner Studienbücher Physik, Stuttgart 1992.

[5] F. Halzen, A. Martin, Quarks and Leptons, John Wiley & Sons, New York.

[6] F. Renard, Basics of e^+e^- collisions, Edition Frontieres, France 1981.

[7] G. Rudolph, Lecture on Particle Physics, University of Innsbruck, Austria, Fall 2001.

[8] G. Marchesini, B.R. Webber, G. Abbiendi, I.G. Knowles, M.H. Seymour and L. Stanco, HERWIGv5 - a Monte Carlo event generator for simulating Hadron Emission Reactions With Interfering Gluons, Computer Phys. Commun. **67** (1992) 465.

[9] B. Andersson and M. Ringner, Bose-Einstein correlations in the Lund model, Nuclear Physics **B513**, 627-644 (1998)

[10] D. Decamp *et al.*, ALEPH collaboration, ALEPH: A Detector for Electron-Positron Annihilations at LEP, Nucl. Instr. Methods **A294** (1990) 121.

[11] D. Buskulic *et al.*, ALEPH collaboration, Performance of the ALEPH detector at LEP, Nucl. Instr. Methods **A360** (1995) 481.

[12] ALEPH in numbers, gathered by D. Schlatter, P. Perrodo, O. Schneider and A. Wagner *alephwww.cern.ch/www3/aleph_general/reports/alephnum/alephnumbers.ps*

[13] G. Batignani *et al.*, 1991 IEEE Nuclear Science Symposium, Santa Fe, IEEE. Trans. Nucl. Sci. NS-39(4/5) (1992) Vol. 1, p. 438.

[14] G.J. Barber *et al.*, Performance of the three-dimensional readout of the ALEPH inner tracking chamber, Nucl. Instr. Methods **A279** (1989) 212.

[15] W.B. Atwood *et al.*, Performance of the ALEPH Time Projection Chamber, Nucl. Instr. Methods **A306** (1991) 446.

[16] ALEPH collaboration, Studies of QCD with the ALEPH detector, Physics Reports **294** (1998) 1.

[17] M.G. Bowler, Bose-Einstein symmetrization, coherence and chaos with particular application to e^+e^- annihilation, TASSO Note No: 342, 15 May 1985.

[18] G.D. Lafferty, Residual Bose-Einstein correlations in inclusive $\pi^+\pi^-$ systems and the $\rho_0(770)$ lineshape in multihadronic Z^0 decay, Z. Phys. **C60** (1993) 659-666.

[19] H.Albrecht, E.Blucher and J. Boucrot, ALPHA User's Guide V125, ALEPH 99-087 SOFTWR 99-001J.

[20] G. Rudolph, ALEPH Collaboration, Global tuning of PYTHIA QCD + Bose-Einstein parameters using Z data, LEP WW workshop, April 2001

[21] V. Kartvelishvili and R. Kvatadze, Event weights for simulating Bose-Einstein correlations, Physics Letters **B514** (2001) 7-18.

[22] L. Lönnblad and T. Sjöstrand, Modelling Bose-Einstein Correlations at LEP 2, Phys. Lett. B351 (1995) 293, Eur. Phys. J. **C2** (1998) 165

[23] G. Rudolph, ALEPH Collaboration, PYTHIA6.1 + BE$_{32}$ tuning in $Z \to q\bar{q}$ and dusc, LEP WW FSI meeting, 30 November 2001.

[24] N. Brown and W.J. Stirling, Jet cross sections at leading double logarithm in e^+e^- annihilation, Phys. Lett. **B252** (1990) 657.

[25] S. Catani, Y.L. Dokshitzer, M. Olsson, G. Turnock, and B.R. Webber, New clustering algorithm for multijet cross sections in e^+e^- annihilation, Phys. Lett. **B269** (1991) 432.

[26] F. Ranjard, The GALEPH Program, *alephwww.cern.ch/LIGHT/galeph.html*

[27] A. Valassi, ALEPH Collaboration, Bose-Einstein correlations in W decays at LEP, XXXth ICHEP, Osaka, 2000.

Curriculum Vitae

Personal Data

Name: Andreas Wildauer
Born: 17th January 1976, Innsbruck, Austria
Parents: Dr. Hermann Wildauer, Brigitte Wildauer
Brother: Dr. Christian Wildauer
Nationality: Austrian

Education

1982-1986	grammar school	Volksschule Innsbruck-Arzl
1986-1992	high school	Bundes(real)gymnasium Innsbruck Sillgasse
1992-1993	high school	Castro Valley High School, California, USA
1993-1995	high school	Bundes(real)gymnasium Innsbruck Sillgasse
June 1995	A-level degree	
1996-now	study of physics	University of Innsbruck
Dec 2001	start of diploma thesis	CERN-ALEPH group, University of Innsbruck

July 1995 - February 1996:   military service in Austria, working as an ambulance man
in the military hospital in Innsbruck

Scholarships

summer 2001	official CERN summerstudent (10 weeks)
autumn 2001	CERN NA48 summerstudent (6 weeks)
summer 2002	CERN NA48 summerstudent (6 weeks)